DEPARTMENT OF THE INTERIOR

U. S. GEOLOGICAL SURVEY

RESPONSE SPECTRUM TECHNIQUES FOR PREDICTING WIND-INDUCED VIBRATIONS AND DISCOMFORT IN HIGH-RISE BUILDINGS

Part 1- Along-wind direction vibrations

E. Şafak
United States Geological Survey
Menlo Park, California, USA

E. Uzgider, *and* A. Şanlı
Istanbul Technical University
Istanbul, Turkey

Open-File Report 90-19

January 1990

TABLE OF CONTENTS

ABSTRACT

Current methods of building design for dynamic wind loads are based on the equivalent static load concept, where the dynamic components of wind loads are converted to an equivalent static load, under which the static deflection is equal to the dynamic deflection. In the equivalent static load approach, accelerations of the building cannot be incorporated in the design, because of their dynamic nature. It is well known, however, that in high-rise buildings wind induced discomfort due to excessive accelerations in the upper stories can be a problem. Thus, there is a need for a design procedure which can include peak accelerations as well as peak displacements.

In this report, we present one such method, the response spectrum method, for predicting the wind-induced dynamic response of high-rise buildings. The technique is similar to that used for earthquake loads, and incorporates not only peak displacements, but also peak accelerations of the building. In this report, only along-wind direction forces and vibrations are considered. The across-wind direction response will be considered in the second part of the research. We develop wind response spectra for a reference building, defined as a single-degree-of-freedom rectangular rigid block with a rotational base spring and a damper. We then show that, for a given building, we can calculate peak modal displacements and accelerations in terms of those of the reference building. We present wind response spectra for different wind and terrain conditions, and perform a parametric analysis to investigate the effect of various parameters on these spectra. We show that existing computer programs that perform spectral analysis for earthquake loads can easily be modified to perform spectral analysis for wind loads.

We also introduce the concept of comfort spectra. For a given building height, we plot the acceleration response spectrum and observe the building frequency corresponding to the critical acceleration for human discomfort. By doing this for a range of building heights, we can construct an interaction curve showing the building height versus critical frequency. We call this interaction curve the comfort spectrum, and present several examples. We conclude by discussing the development of a single design spectrum for earthquake and wind loads.

ACKNOWLEDGMENT

This research has been partially financed by the NATO Collaborative Grants Programme under Grant No 0121/88. The authors wish to acknowledge the support they received from NATO.

1. INTRODUCTION

Wind loading is one of the most important factors to be considered in designing high-rise buildings. The dynamic component of wind forces have long been recognized and incorporated in design codes. The current practice of design for wind is based on the equivalent static load concept, where the dynamic component of the wind load is converted to an equivalent static load, under which the static deflection of the building is equal to the dynamic deflection (ANSI, 1982; NBCC, 1985). This load, along with the static component of wind load, is applied to the building, and a static analysis is performed for design. This approach is known as the gust factor approach (Davenport, 1961). The design criterion for the gust factor method is to limit the stresses and deflections, the same as for any other static load, since the method is based on the equivalent static load concept. It is well known, however, that one of the major problems in high-rise buildings is the wind-induced discomfort of occupants. Occupant discomfort occurs due to excessive accelerations, rather than deflections. This observation suggests that the wind design criterion of high-rise buildings should be based on peak accelerations, as well as peak displacements. Current codes do not have any provisions for wind-induced peak accelerations. Using existing theory, analytical expressions can be developed for peak accelerations (e.g., Simiu and Scanlan, 1978; Şafak and Foutch, 1987). However, the expressions are probably too complex to use for practicing design engineers. There is a need for a simple wind design methodology that will not only incorporate peak displacements and peak accelerations but also will be consistent with the current methods of analysis, so that design engineers can easily adopt it.

One such method is the response spectrum method. The response spectrum method has been widely used for earthquake design, and is well known among engineers. It is very simple, and can incorporate peak accelerations, velocities, and displacements. It was first suggested by Newmark (1966), and Cevallos-Candau (1980) showed that the earthquake and wind loads, and corresponding building responses, have a lot of similarities. Therefore, similar methods of analysis, such as the response spectrum technique, can be used for both loads. An important advantage of using the response spectrum technique for both wind and earthquake loads is that when both loads need to be considered for design, the designer would know beforehand which load will dominate his design, without doing a separate analysis for each load.

In this report, we present the response spectrum technique for predicting wind-induced response of high-rise buildings. The technique is similar to that used for earthquake loads, and incorporates not only peak displacements, but also peak accelerations of the building. Therefore, the method can be used for design for safety (i.e., considers peak displacements), and also for design for comfort (i.e., considers peak accelerations). We first outline current

techniques used for wind and earthquake response analysis of structures. We then show how the random vibration technique used for wind loads can be put into a response spectrum form. We present wind response spectra for different wind and terrain conditions, and perform a parametric analysis to investigate the effect of various parameters on spectra. We show that existing computer programs that perform spectral analysis for earthquake loads can easily be modified to also perform spectral analysis for wind loads. We introduce a comfort spectrum, by which a designer can determine whether the building will be susceptible to wind-induced discomfort. We conclude by investigating the feasibility of developing a single design spectum for wind and earthquake forces.

2. WIND FORCES ON HIGH-RISE BUILDINGS

Wind-induced vibrations in high-rise buildings are due to individual or combined effects of the following dynamic force mechanisms: along-wind forces due to turbulence, across-wind forces due to vortex shedding, wake buffeting, and galloping. Along-wind forces are in the direction of main wind flow. They include static and dynamic components, generated by the steady and fluctuating components of the wind, respectively, and are the most dominant force mechanism in a typical building. In general, along wind forces are in the form of pressures on the frontal (i.e., windward) face, and suctions on the back (i.e., leeward) face of the building. Across-wind forces are generated by vortecies that develop at the sides of the building moving clockwise and counterclockwise, and shed in an alternating fashion in the direction perpendicular to the mean wind flow. Across-wind forces can be critical for slender structures, such as buildings with very large height to width ratios, smokestacks, and transmission towers. Wake buffeting occurs if one structure is located in the wake of another structure, and can cause large oscillations in the downstream structure if the two structures are similar in shape and size, and less than ten-diameter apart. Galloping is an oscillation induced by forces generated by the motion itself. It corresponds to an unstable motion with negative damping, and can be seen in structures like transmission lines, or long slender towers with sharp edged crossections. More detail on wind force mechanisms can be found in Simiu and Scanlan (1978) and Şafak and Foutch (1980). In this study, we will deal only with along-wind forces in the direction of main wind flow. Forces in the across-wind direction will be considered in the second phase of the study.

2.1. Models of wind velocity near ground:

Wind velocity generates all the force mechanisms acting on the structure. Near the ground, the wind velocity $V(z,t)$ at height z can be expressed as the sum of two components, as shown in Fig. 1, such that

$$V(z,t) = V_0(z) + w(z,t) \tag{1}$$

$V_0(z)$ is called the mean (i.e., average) wind velocity, and is time-invariant. $w(z,t)$ is the fluctuating part of the wind velocity, superimposed over the mean part. The variation of $V_0(z)$ with height z is known as the *velocity profile*. The velocity profile starts from zero at $z = 0$ (i.e., the ground surface) and increases to a constant level at the height where there is no influence of surface friction on the velocity. This height is known as the *gradient height*, and the corresponding constant velocity is known as the *gradient velocity*.

There are two widely-used models for velocity profiles, the power-law model, and the logarithmic model. The power-law model is given by the following equation (Davenport, 1961):

$$V_0(z) = V_0(z_r)\Big(\frac{z}{z_r}\Big)^{\alpha} \tag{2}$$

where $V_0(z_r)$ is the mean wind velocity at the reference height z_r, and α is the exponent. The standard value for the reference height is $z_r = 10\ m$. The power law can also be expressed in terms of the gradient height z_G and gradient velocity $V_0(z_G)$ by replacing z_r and $V_0(z_r)$ in Eq.2 by z_G and $V_0(z_G)$. Both z_G and α depend on the roughness of the terrain. Suggested values for z_G and α are $z_G = 700, 900, 1200, 1500$ feet, and $\alpha = 0.10, 0.14, 0.22, 0.33$ for open water, open country, suburban terrain, and center of large cities, respectively.

The logarithmic model of wind velocity is defined by the following equation (Simiu, 1973):

$$V_0(z) = V_0(z_r) \cdot \frac{\ln(z/z_0)}{\ln(z_r/z_0)} \tag{3}$$

where z_0 is called the roughness length. Approximate roughness lengths for various terrains are $z_0 = 0.005, 0.007, 0.30, 1.00, 2.50$ in meters for open water, open terrain, sparsely built-up suburbs, densely built-up suburbs, and center of large cities, respectively.

The fluctuating component $w(z,t)$ of wind velocity is random. A widely used assumption is that $w(z,t)$ is a zero-mean, stationary, Gaussian random process with a specified power spectral density function (PSDF). As with the velocity profile, there are also two different forms suggested for the spectrum of $w(z,t)$ (also known as the turbulence spectrum). The earlier form suggested by Davenport (1961) is given by the equation

$$S_w(f) = 4K \cdot \frac{V_0^2(10)}{f} \cdot \frac{X^2}{(1+X^2)^{4/3}} \quad \text{with} \quad X = \frac{1200f}{V_0(10)} \tag{4}$$

where $V_0(10)$ is the mean wind velocity in meters per second at the reference height of 10 meters, f is the frequency in cycles per second (Hz), and K is the surface drag coefficient. The value of K varies from 0.005 for open country to 0.05 for city centers. The shape of Davenport's spectrum is independent of the height, and has a peak at a wave length of 600 meters (i.e., $V_0(10)/f = 600$). This spectrum is currently used in building codes in many countries.

A later model for the turbulence spectrum is suggested by Simiu (1974), and can incorporate the variation of the spectrum with height. Simiu's spectrum is given by the following equation:

$$S_w(z,f) = \frac{u_*^2}{f} \cdot \frac{200N}{(1+50N)^{5/3}} \quad \text{with} \quad N = \frac{fz}{V_0(z)} \tag{5}$$

where u_* is known as the friction velocity, calculated in terms of the reference velocity and the roughness length by the following equation

$$u_* = \frac{V_0(z_r)}{2.5\ln(z_r/z_0)} \tag{6}$$

Since N in Eq.5 is a function of z, $S_w(z,f)$ is height dependent. A more precise, but analytically more complicated, form of this spectrum is given in Simiu (1974).

The level of turbulence in a wind flow is described by its turbulence intensity. The turbulence intensity $I(z)$ is calculated as the ratio of the RMS (root-mean-square) value of the fluctuating component of wind velocity to the mean component. That is

$$I(z) = \frac{\sigma_w(z)}{V_0(z)} \tag{7}$$

where $\sigma_w(z)$ is the RMS value of $w(z,t)$. From random process theory,

$$\sigma_w^2(z) = \int_{f=0}^{\infty} S_w(z,f)df \tag{8}$$

For Davenport's spectrum (Eq.4), σ_w is constant, since the spectrum is independent of z, and equal to $6KV_0^2(10)$. For tall buildings, the turbulence intensity may vary from 0.05 to 0.30 depending on the building height and the roughness of the terrain.

2.2. Wind forces in the along-wind direction:

Forces in the along-wind direction are generated by the velocity of the wind flow. Neglecting the relatively small added mass term, the pressure $P(z,t)$ acting at a point of height z of a fixed body in a turbulent flow can be written as

$$P(z,t) = \frac{1}{2}\rho C_p(z) V^2(z,t) \tag{9}$$

where $V(z,t)$ is the wind velocity, $C_p(z)$ is called the pressure coefficient, and ρ is the mass density of the air. By separating the wind velocity $V(z,t)$ into its mean and fluctuating components, as in Eq.1, and also neglecting the $w^2(z,t)$ terms, Eq.9 can be approximated as

$$P(z,t) \approx \frac{1}{2}\rho C_p(z) V_0^2(z) + \rho C_p(z) V_0(z) w(z,t) \tag{10}$$

The omision of the $w^2(z,t)$ term is justified since the turbulence intensity is generally much less than one. The first term on the right hand side of Eq. 10 is independent of t, therefore it represents the static wind pressure. The second term is the dynamic wind pressure. Denoting static and dynamic wind pressures by $P_0(z)$ and $p(z,t)$, respectively, we can write

$$P(z,t) = P_0(z) + p(z,t) \tag{11}$$

where

$$P_0(z) = \frac{1}{2}\rho C_p(z) V_0^2(z) \quad \text{and} \quad p(z,t) = \rho C_p(z) V_0(z) w(z,t) \tag{12}$$

Since $P_0(z)$ is a static load, the response of the structure resulting from this load can be calculated by using static methods of analysis.

The calculation of the response due to the dynamic pressure $p(z,t)$ requires the application of random vibration techniques because of the random $w(z,t)$. Since $p(z,t)$ is a linear function of $w(z,t)$, we conclude that $p(z,t)$ is also a zero-mean, stationary, Gaussian random variable. Its standard deviation, $\sigma_p(z)$, and PSDF, $S_p(z,f)$, can be calculated in terms of those of $w(z,t)$:

$$\sigma_p(z) = \rho C_p(z) V_0(z) \sigma_w(z) \tag{13}$$

and

$$S_p(z,f) = \left[\rho C_p(z) V_0(z)\right]^2 S_w(z,f) \tag{14}$$

$S_p(z,f)$ is sufficient to describe fully the stochastic characteristics of $p(z,t)$.

3. DYNAMIC RESPONSE OF HIGH-RISE BUILDINGS

Vibration tests indicate that the behavior of high-rise buildings under dynamic loads is somewhere between that of a shear beam and a flexural beam. The closed form vibration equations, assuming a shear beam or a flexural beam model, can be derived in the continuous domain (see, for example Şafak and Foutch, 1980). Vibration equations can also be expressed in a discrete domain by using discrete modeling techniques, such as matrix methods and finite element methods. We will prefer the discrete approach, so that we can make use of commercially available computer programs.

We will assume that the motion of the building can be modeled in terms of horizontal displacements at each story level. The rotations will be neglected, since their contribution to the response is generally very small (Hurty and Rubinstein, 1964). We will also assume that the building is symmetric, and moves only in the along-wind direction (we will consider the motion in the across-wind direction in the second phase of the study). With these assumptions, the building becomes an n-DOF (n-degrees-of-freedom) dynamic system, n representing the number of stories. The equations of motion, assuming linear behavior, can be written as

$$[M]\{\ddot{y}(t)\} + [C]\{\dot{y}(t)\} + [K]\{y(t)\} = \{F(t)\} \tag{15}$$

In Eq.15, $[M]$, $[C]$, and $[K]$ are $n \times n$ mass, damping, and stiffness matrices, respectively, and $\{y(t)\}$ and $\{F(t)\}$ are n-dimensional displacement and force vectors. The dots over y denote derivatives with respect to time t. The solution of Eq.15 can be accomplished by using modal analysis techniques. First, assuming that $[C] = 0$ and $\{F(t)\} = 0$ in Eq.15, we solve the following n-dimensional eigenvalue equation:

$$[M]\{\ddot{y}(t)\} + [K]\{y(t)\} = 0 \tag{16}$$

Eigenvalues and eigenvectors obtained from the solution of this equation correspond, respectively, to n natural frequencies and mode shapes of the building. Using calculated mode shapes, the displacement vector $\{y(t)\}$ can be expressed as

$$\{y(t)\} = [\Phi]\{q(t)\} \tag{17}$$

where $[\Phi]$ is a $n \times n$ matrix composed of mode shapes (i.e., each column of $[\Phi]$ represents a mode shape), and $\{q(t)\}$ is the n-dimensional generalized coordinate vector representing the modal amplitudes. In explicit form, the i-th component $y_i(t)$ of $\{y(t)\}$ can be written

$$y_i(t) = \sum_{k=1}^{n} \Phi_{ik} q_k(t) \tag{18}$$

where Φ_{ik} represents the element at the i-th row and k-th column of matrix $[\Phi]$. An important property of vibration mode shapes of an n-DOF system is orhogonality:

$$\{\Phi_k\}^T[M]\{\Phi_l\} = 0 \quad \text{and} \quad \{\Phi_k\}^T[K]\{\Phi_l\} = 0 \quad \text{for} \quad k \neq l \tag{19}$$

where $\{\Phi_k\}$ and $\{\Phi_l\}$ are vectors denoting the k'th and l'th mode shapes, and the superscript T denotes the transpose. If it is assumed that the damping matrix C is a linear combination of mass and stiffness matrices (i.e., $C = c_m M + c_k K$), the orthogonality property also applies to the damping matrix, that is

$$\{\Phi_k\}^T[C]\{\Phi_l\} = 0 \quad \text{for} \quad k \neq l \tag{20}$$

The orthogonality property can be used to reduce the n-dimensional matrix equation in Eq.15 to a set of n independent modal equations. Using Eq.17 in Eq.15, and then multiplying both sides by the transpose of any (e.g., k-th) mode shape vector, and also using the orthogonality properties (Eqs.19 and 20), we can write for the k-th modal equation of the motion

$$\{\Phi_k\}^T[M]\{\Phi_k\}\{\ddot{q}(t)\} + \{\Phi_k\}^T[C]\{\Phi_k\}\{\dot{q}(t)\} + \{\Phi_k\}^T[K]\{\Phi_k\}\{q(t)\} = \{\Phi_k\}^T\{F(t)\} \tag{21}$$

For simplicity, introduce the following notation:

$$M_k^* = \{\Phi_k\}^T[M]\{\Phi_k\} \tag{22}$$

$$C_k^* = \{\Phi_k\}^T[C]\{\Phi_k\} \tag{23}$$

$$K_k^* = \{\Phi_k\}^T[M]\{\Phi_k\} \tag{24}$$

$$F_k^*(t) = \{\Phi_k\}^T\{F(t)\} \tag{25}$$

M_k^*, C_k^*, K_k^*, and $F_k^*(t)$ are called the k-th generalized mass, damping, stiffness, and force, respectively. To simplify it further, we will write

$$C_k^* = 2\xi_{0k}(2\pi f_{0k})M_k^* \quad \text{and} \quad K_k^* = (2\pi f_{0k})^2 M_k^* \tag{26}$$

where ξ_{0k} is the damping ratio, and f_{0k} is the cyclic frequency for the k-th mode. With these, we can write for the k-th modal equation of the motion as

$$\ddot{q}_k(t) + 2\xi_{0k}(2\pi f_{0k})\dot{q}_k(t) + (2\pi f_{0k})^2 q_k(t) = \frac{F_k^*(t)}{M_k^*} \tag{27}$$

Eq.27 is equivalent to the equation of a single degree of freedom system. The solution can be written, by using the Duhamel's integral, as

$$q_k(t) = \frac{1}{M_k^*(2\pi f_{0dk})} \int_{\tau=0}^{t} F_k^*(\tau)\, h_k(t-\tau)\, d\tau \tag{28}$$

$h_k(t-\tau)$ is the impulse response function for the k-th mode, and is calculated by the following equation

$$h_k(t-\tau) = e^{-\xi_{0k}(2\pi f_{0k})(t-\tau)} \sin[(2\pi f_{0dk})(t-\tau)]\, d\tau \tag{29}$$

where f_{0dk} is the damped natural frequency given as $f_{0dk} = f_{0k}\sqrt{1-\xi_{0k}^2}$.

The total response is obtained by combination of modal responses according to Eq.17.

4. RESPONSE TO WIND LOADS

We have presented equations to calculate the dynamic response of a high-rise building to an arbitrary load. To calculate the response for wind loads we first have to determine the wind load vector by integrating the wind pressures given by Eq.9 over the dimensions, i.e., the wind exposure area, of the building. As mentioned earlier, we will assume that wind blows perpendicular to one of the faces of the building, and consider only the along-wind direction forces at this stage of the study. We will also assume that the pressures on the windward and leeward faces are fully correlated, and the pressure coefficient used represents the sum of the averaged (over the width of the building) pressure coefficients on the windward and leeward faces of the building. Because they are averaged values across the width, the pressure coefficients will vary only with height. With these, we can write the j-th component of the wind force vector $\{P_w(t)\}$ as

$$P_{wj}(t) = \int\int_{A_j} \left[\frac{1}{2}\rho C_p(z) V_0^2(z) + \rho C_p(z) V_0(z) w(x,z,t)\right] dxdz \tag{30}$$

where A_j denotes the tributary wind exposure area for the j-th story, and x denotes the horizontal coordinate axis perpendicular to the main wind flow. It is assumed that $V_0(z)$ does not change in the horizontal direction. The tributary area A_j can be calculated as

$$A_j = B_j \frac{h_{j+1} + h_j}{2} \tag{31}$$

B_j and h_j are the width and the story height (with respect to the story below), respectively, at the j'th story.

$\{P_w(t)\}$ can be separated into static and dynamic components, $\{P_{0w}\}$ and $\{p_w(t)\}$, such that

$$\{P_w(t)\} = \{P_{0w}\} + \{p_w(t)\} \tag{32}$$

The j'th components of $\{P_{0w}\}$ and $\{p_w(t)\}$ can be written, from Eq.30, as

$$P_{0wj} = \frac{1}{2}\rho B_j \int_{z_j - h_j/2}^{z_j + h_{j+1}/2} C_p(z) V_0^2(z)\, dz \tag{33}$$

$$p_{wj}(t) = \rho \int\int_{A_j} C_p(z) V_0(z) w(x, z, t)\, dx dz \tag{34}$$

All the other components can be calculated similarly.

Since $\{P_{0w}\}$ is a static load, the resulting static response, $\{y_0\}$, can easily be calculated as

$$\{y_0\} = [K]^{-1}\{P_{0w}\} \tag{35}$$

For the dynamic response, we will first calculate the generalized force vector $\{F^*(t)\}$. For the j'th component of $\{F^*(t)\}$, we can write from Eq.25 that

$$F_j^*(t) = \{\Phi_j\}^T\{p_w(t)\} = \sum_{k=1}^{n} \Phi_{jk} p_{wk}(t) \tag{36}$$

where the vector $\{\Phi_j\}$ denotes the j'th mode shape. In Eq.36, the generalized force is given in a discrete form as the sum of modal amplitudes multiplied by the corresponding dynamic story forces (i.e., dynamic pressures times the tributary story area). The same equation can also be written in a continuous form by using integrals instead of sums. We will prefer the

continuous form, since the available information on the stochastic description of dynamic wind loads is all given in the continuous domain. When the mode shapes are available only in discrete form, we can approximate the continuous mode shapes by connecting the discrete amplitudes by straight lines. Using Eq.34, we can write for the j'th generalized modal wind force in the continuous form as

$$F_j^*(t) = \int\int_{A_j} \Phi_j(z)\, \rho C_p(z) V_0(z) w(x,z,t)\, dxdz \tag{37}$$

where $\Phi_j(z)$ denotes the continuous j'th mode shape.

Since $w(x,z,t)$ is random, the generalized modal force $F_j(t)$ is also random. Therefore, the calculation of the response requires applications of random vibration techniques. One popular method for stationary excitations is the spectral analysis technique, where the response is calculated in terms of PSDF's. For a multi-degree-of-freedom system (e.g., Eq.15) with random excitation, the relationship between input and output PSDF's can be written as (Lin, 1976)

$$S_y(z_1,z_2,f) = \{\Phi(z_1)\}[H(f)][S_{F^*}(f)][\bar{H}(f)]^T\{\Phi(z_2)\}^T \tag{38}$$

$S_y(z_1,z_2,f)$ is the cross-PSDF of the responses at points z_1 and z_2, and $[S_{F^*}(f)]$ is the PSDF matrix of the generalized force. $\{\Phi(z_1)\}$ and $\{\Phi(z_2)\}$ denote vectors composed of modal coordinates at height z_1 and z_2, respectively.

$[H(f)]$ is the complex frequency response matrix of the structure, calculated by the equation

$$[H(f)] = \left[-(2\pi f)^2[M^*] + \mathbf{i}(2\pi f)[C^*] + [K^*]\right]^{-1} \tag{39}$$

where $\mathbf{i}= \sqrt{-1}$. $[\bar{H}(f)]$ denotes the complex conjugate of $[H(f)]$.

The j,k component of the PSDF matrix $[S_{F^*}(f)]$ of the generalized force can be written in the continuous domain from Eq.37 as

$$S_{F^*jk}(f) = \int\int_{A_j}\int\int_{A_k} \Phi_j(z_1)\Phi_k(z_2)\rho^2 C_p(z_1)C_p(z_2)V_0(z_1)V_0(z_2) \\ S_w(x_1,z_1,x_2,z_2,f)\, dx_1 dz_1 dx_2 dz_2 \tag{40}$$

$S_w(x_1,z_1,x_2,z_2,f)$ is the cross-PSDF of the fluctuating wind velocitiy $w(x,z,t)$, and can be written as

$$S_w(x_1, z_1, x_2, z_2, f) = S_w^{1/2}(z_1, f) S_w^{1/2}(z_2, f) Coh(x_1, z_1, x_2, z_2, f) \tag{41}$$

where $S_w(z, f)$ is the PSDF at z, and $Coh(x_1, z_1, x_2, z_2, f)$ is the coherence function of the fluctuating wind velocities at points (x_1, y_1) and (x_2, y_2). It is assumed that $S_w(z, f)$ does not change horizontally (i.e., it is not a function of x). The equation suggested for $Coh(x_1, z_1, x_2, z_2, f)$ is (Vickery, 1971)

$$Coh(x_1, z_1, x_2, z_2, f) = \exp\left[-2f \frac{\left[C_x^2(x_1 - x_2)^2 + C_z^2(z_1 - z_2)^2\right]^{1/2}}{V_0(z_1) + V_0(z_2)}\right] \tag{42}$$

C_x and C_z are called the exponential decay coefficients. Their suggested values are $C_x = 16$ and $C_z = 10$. Experiments show that these values can change significantly, depending on the terrain, height, and the wind speed, and therefore represent a source of uncertainity (Simiu and Scanlan, 1978).

By using expressions derived in Eqs.39-42, the response PSDF, $S_y(z_1, z_2, f)$, is calculated from Eq.38. The integral of $S_y(z_1, z_2, f)$ over the frequency f gives the covariance matrix, $\sigma_y^2(z_1, z_2)$, of the response. That is

$$\sigma_y^2(z_1, z_2) = \int_0^\infty S_y(z_1, z_2, f)\, df \tag{43}$$

For $z_1 = z_2 = z$, $\sigma_y^2(z)$ is the mean square response at z. At a given height z, the peak response is calculated as

$$\max_t y(z, t) = y_0(z) + g_y(z)\sigma_y(z) \tag{44}$$

where $y_0(z)$ is the static response due to static wind load, and $g_y(z)$ is known as the peak (or gust) factor. The peak factor can approximately be calculated by the following equation (Davenport, 1964):

$$g_y(z) = \sqrt{2 \ln \nu(z) T} + \frac{0.577}{\sqrt{2 \ln \nu(z) T}} \tag{45}$$

$\nu(z)$ is the average number of peaks in the response $y(z)$ per unit time, and T is the duration in seconds considered for the excitation and response in peak calculations. A commonly used value for T is 3600 seconds, corresponding to a one-hour wind storm. $\nu(z)$ can be calculated in terms of the PSDF by the equation

$$\nu^2(z) = \frac{\int_0^\infty f^2 S_y(z,f)\,df}{\int_0^\infty S_y(z,f)\,df} \tag{46}$$

This approximation is based on the assumption that the response is a narrow band stationary random process with independently arriving peaks.

The accelerations can be calculated by taking the second derivatives of displacements. The PSDF $S_a(z_1, z_2, f)$ of accelerations can be written in terms of the PSDF of displacements as

$$S_a(z_1, z_2, f) = (2\pi f)^4 S_y(z_1, z_2, f) \tag{47}$$

The covariance function of the accelerations is

$$\sigma_a(z_1, z_2) = \int_0^\infty S_a(z_1, z_2, f)\,df \tag{48}$$

The peak acceleration at height z is calculated in the same way as the peak displacements (Eq.44):

$$\max_t a(z,t) = g_a \sigma_a(z) \tag{49}$$

Note that the mean (i.e., static) acceleration is zero. g_a is calculated similar to g_y by replacing σ_y and S_y in Eqs.44-46 by σ_a and S_a.

5. RESPONSE SPECTRA FOR EARTHQUAKE LOADS

The response spectrum for earthquakes is a curve that shows the variation of the peak displacement of a SDOF (single-degree-of-freedom) oscillator with its natural frequency for a specifed damping ratio and earthquake excitation. If a SDOF oscillator is subjected to an earthquake described by the base acceleration $a_g(t)$, as schematically shown in Fig. 2, we can write from the equilibrium condition that the sum of inertia, damping, and elastic forces are zero

$$M_0 \ddot{y}_0(t) + C_0 \dot{y}_0(t) + K_0 y_0(t) = -M_0 a_g(t) \tag{50}$$

where $y_0(t)$ corresponds to the relative displacement of the oscillator with respect to ground, M_0, C_0, and K_0 are the mass, damping, and the stiffness of the oscillator. In

terms of the natural frequency and damping, we can write the same equation (see Eq.26) as

$$\ddot{y}_0(t) + 2\xi_0(2\pi f_0)\dot{y}_0(t) + (2\pi f_0)^2 y_0(t) = -a_g(t) \tag{51}$$

Equation 50 shows that the effect of earthquake base motion in a SDOF oscillator is equivalent to applying a ficticious force on the oscillator, defined by the equation

$$F_0(t) = -M_0 a_g(t) \tag{52}$$

Using Duhamel's integral, as in Eq.28, we can write for the displacement (relative to the base) $y_0(t)$ of a SDOF oscillator to earthquake base acceleration $a_g(t)$

$$y_0(t) = -\frac{1}{2\pi f_{0d}} \int_{\tau=0}^{t} a_g(\tau)\, h_0(t-\tau)\, d\tau \tag{53}$$

where $h_0(t-\tau)$ is given by Eq.29. We define the response spectrum $D(f_0)$ for frequency f_0 as

$$D(f_0) = \max_t y_0(t) \tag{54}$$

The plot of $D(f_0)$ with respect to f_0 gives the response spectral curve. Since the response $y_0(t)$ is dependent on the damping in addition to the excitation, different damping ratios, ξ_0, and excitations, $a_g(t)$, would give different spectral curves.

For multi-story buildings, again considering the relative displacement of the building with respect to the ground, we can express the load vector as the product of the mass matrix and acceleration vector whose elements are all equal to ground acceleration. That is,

$$\{F(t)\} = -[M]\{I\}a_g(t) \tag{55}$$

where $\{I\}$ denotes an n-dimensional unit vector. The generalized force vector given by Eq.25 then becomes

$$F_k^*(t) = -\Phi_k^T M I a_g(t) = \lambda_k a_g(t) \quad \text{where} \quad \lambda_k = -\Phi_k^T M I \tag{56}$$

λ_k is called the participation factor for the k-th mode, which represents the portion of total load associated with that mode. Using Eq.56 in Eq.28, we can write for the k-th modal response $q_k(t)$ of a building subjected to ground acceleration $a_g(t)$

$$q_k(t) = \frac{\lambda_k}{M_k^*} \frac{1}{2\pi f_{0dk}} \int_{\tau=0}^{t} a_g(\tau)\, h_k(t-\tau)\, d\tau \tag{57}$$

By comparing Eq.57 with Eq.53, we note that the right hand side of Eq.57 is equivalent to the response of a SDOF oscillator except the constant term λ_k/M_k^*. Therefore the peak k'th modal response is equal to that of a SDOF oscillator corresponding to mode k (i.e., the amplitude of the response spectrum for damping ξ_{0k} at frequency f_{0k}) multiplied by λ_k/M_k^*. That is

$$\max_t q_k(t) = \frac{\lambda_k}{M_k^*} \cdot \max_t y_0(t) = \frac{\lambda_k}{M_k^*} \cdot D(f_{0k}) \tag{58}$$

For each mode, peak modal responses can be calculated similarly by using the response spectrum. Although the response at any given time can be written in terms modal responses (Eq.17), the same is not true for the peak response, because the peak modal responses do not necessarily occur at the same time. In other words, the peak response is not equal to, but less than, the sum of peak modal responses. Various methods have been used to approximate peak response in terms of peak modal responses, such as the absolute sum, the square root of the sum of the squares, or the quadratic combination.

6. RESPONSE SPECTRA FOR WIND LOADS

Development of response spectra for wind loads can be accomplished following a similar approach to that for earthquake loads. Wind response spectra should be defined for a given site, since the velocity and turbulence structure of the wind is strongly site dependent. Earthquake loads are inertia loads. Therefore the spectral response involves only the damping and the natural frequency of a structure and not any other structural parameter. Wind loads, however, are strongly dependent on the outside geometry of the structure. It is the size and the shape of the wind exposure area that determine the total wind load on the building. Therefore, wind response is dependent not only on the natural frequency and damping, but also on the outside geometry of the structure. Since we are dealing with buildings with rectangular cross-sections and normally incident wind, and also considering only along-wind vibrations at this phase of the study, we can define the outside geometry with the height and frontal width of the building. Further simplification can be achieved for very tall buildings by neglecting the variation of wind pressures in the horizontal direction and using pressure coefficients averaged over the frontal width. For such buildings, the outside geometry is represented only by the height of the building. In the formulation that follows we will consider both the height and the width of the building. We will define

wind response spectra for a given site, and given structural damping, height, and height-to-width ratio. The dependence of wind response spectra on height and height-to-width ratio is the major difference when compared to earthquake response spectra.

6.1. A reference building for wind spectra:

In order to develop wind response spectra, we will consider a reference building as schematically shown in Fig. 3. The reference building can be visualized as a rigid block of specified width, height, and mass, connected to the base by a rotational spring-dashpot system. Therefore, the reference system is a SDOF system, and its single mode shape is a straight line. We will develop wind response spectra for the reference system for different damping ratios, wind velocities, heights, and height-to-width ratios. We will assume unit mass per unit height, and a location in the middle of a city.

Using the coordinate system shown in Fig. 3, we can write for the response of the reference system as

$$y_r(z,t) = \Phi_r(z) q_r(t) \tag{59}$$

where $\Phi_r(z)$ denotes the single mode shape of the system. Since the building has only one degree of freedom, a rigid body rotation with respect to the base, we can write for the mode shape

$$\Phi_r(z) = \frac{z}{H} \tag{60}$$

The equation for $q_r(t)$, similar to Eq.28, is

$$\ddot{q}_r(t) + 2\xi_{0r}(2\pi f_{0r})\dot{q}_r(t) + (2\pi f_{0r})^2 q_r(t) = \frac{F_r^*(t)}{M_r^*} \tag{61}$$

where ξ_{0r} and f_{0r} are the damping ratio and natural frequency, and F_r^* and M_r^* are the generalized load and mass of the reference building, respectively. For unit mass per unit height, we can calculate the generalized mass of the reference system as

$$M_r^* = \int_0^H \Phi_r^2(z) \cdot 1 \cdot dz = \int_0^H \left(\frac{z}{H}\right)^2 dz = \frac{H}{3} \tag{62}$$

Using Eqs.38-41, we can write for the PSDF, $S_{y_r}(z_1, z_2, f)$, of the displacement response of the reference system

$$S_{y_r}(z_1, z_2, f) = \Phi_r(z_1)\Phi_r(z_2)|H(f)|^2(\rho C_D B)^2 V_0(z_1)V_0(z_2) \\ S_w^{1/2}(z_1, f)S_w^{1/2}(z_2, f)Coh(z_1, z_2, f) \qquad (63)$$

The PSDF for the accelerations is

$$S_{a_r}(z_1, z_2, f) = (2\pi f)^4 S_{y_r}(z_1, z_2, f) \qquad (64)$$

The RMS displacement $\sigma_{yr}(H)$, and the RMS acceleration $\sigma_{ar}(H)$ at the top of the building are

$$\sigma_{yr}(H) = \int_0^\infty S_{y_r}(H, f)\, df \qquad \text{and} \qquad \sigma_{ar}(H) = \int_0^\infty S_{a_r}(H, f)\, df \qquad (65)$$

For the peak displacement, $\max_t y_r(H, t)$, and the peak acceleration $\max_t a_r(H, t)$, at the top, we can write (see, Eqs.44-49)

$$\max_t y_r(H, t) = y_{0r}(H) + g_{yr}(H)\sigma_{yr}(H) \qquad (66)$$

$$\max_t a_r(H, t) = g_{ar}(H)\sigma_{ar}(H) \qquad (67)$$

where $y_{0r}(H)$ is the static displacement due to static wind load, and $g_{yr}(H)$ and $g_{ar}(H)$ are the displacement and acceleration peak factors, respectively, at the top of the reference system.

For the displacement response spectra, we will only consider the dynamic displacement, since the static displacement can easily be calculated using static analysis. It should be noted here that, if desired, the static displacement can also be included in the response spectrum by expanding it into static modal components. We will define the displacement response spectra as the plot of the peak dynamic displacement response at the top of the reference building against the natural frequency for a range of frequencies. Therefore, for the natural frequency f_{0j} the displacement spectra, $D(f_{0j})$, is

$$D(f_{0j}) = \max_t \Big[y_r(H, t)\Big]_{dynamic} = g_{yr}(H)\sigma_{yr}(H) \qquad (68)$$

Similarly for the acceleration spectra, we can write

$$A(f_{0j}) = \max_t a_r(H,t) = g_{ar}(H)\sigma_{ar}(H) \tag{69}$$

6.2. Modal participation factors for wind spectra:

In order to calculate the wind response of a given building by using the response spectra of the reference building, we first have to determine the modal participation factors. The modal participation factor will be defined as the ratio of the peak modal response of a given system to that of the reference system that has the same modal frequency and damping.

The PSDF, $S_{yj}(f)$, of the j-th modal displacement of a given building is (from Eq.38)

$$S_{yj}(z,f) = \Phi_j^2(z)|H_j(f)|^2 S_{F_j^*}(f) \tag{70}$$

where $H_j(f)$, the frequency response function for the j-th mode, can be written from Eq.39

$$H_j(f) = \frac{1}{M_j^*\left[-(2\pi f)^2 + \mathbf{i}(2\pi f)(2\xi_{0j})(2\pi f_{0j}) + (2\pi f_{0j})^2\right]} \tag{71}$$

$S_{F_j^*}(f)$ can be calculated from Eq.40 by putting $j = k$. Similarly, the PSDF of the reference system, $S_{rj}(f)$, corresponding to j-th mode (i.e., the reference system with frequency f_{0j}, damping ξ_{0j}, and same outside dimensions) is

$$S_{rj}(z,f) = \Phi_r^2(z)|H_{rj}(f)|^2 S_{F_{rj}^*}(f) \tag{72}$$

The frequency response function of the reference system, H_{rj}, is the same as that of the actual system for the j'th mode, $H_j(f)$, except the scaling factor (i.e., the mass term). The relationship can be written as

$$H_{rj}(f) = \frac{M_r^*}{M_j^*} \cdot H_j(f) \tag{73}$$

Since the loading on the reference and actual systems are the same, and their frequency response functions are equal to within a scaling factor, we conclude that the spectral contents of the modal response and the response of the corresponding reference system are the same. Therefore the peak factors for each response can be assumed equal. Consequently, the ratio of the peak modal response to the peak response of the corresponding reference system is equal to the ratio of their RMS responses. If we denote this ratio by $k_j(z)$ for the responses at height z, we can write

$$k_j^2(z) = \frac{\sigma_{yj}^2(z)}{\sigma_{rj}^2(z)} = \frac{\int_0^\infty S_{yj}(z,f)\,df}{\int_0^\infty S_{rj}(z,f)\,df} \tag{74}$$

Because of the four-fold integration involved in the calculations of $S_{F_j^*}(f)$ and $S_{F_{rj}^*}$ (see Eq.40), a straightforward evaluation of $k_j(z)$ is very complicated, and would not have much practical use. To simplify the calculations, we will consider two extreme cases regarding the spatial correlation of the pressures. Case 1 will refer to the situation where the pressures are spatially uncorrelated, whereas Case 2 will refer to the situation where the pressures are fully correlated. In addition, we will assume that the PSDF of the velocity fluctuations is independent of the height as suggested by Davenport (1961). The simplifed expressions for $k_j(z)$ can then be developed as follows:

6.2.1. Case 1: Pressures are spatially uncorrelated

If the pressures are uncorrelated we can assume that

$$Coh(x_1, z_1, x_2, z_2, f) = \delta(x_1 - x_2)\delta(z_1 - z_2) \tag{75}$$

where δ denotes the Dirac's delta function. Using this expression, and the assumption that $S_w(f)$ is independent of z, it can be shown from Eq.40 that

$$S_{F_j^*}(f) = (\rho B_j)^2 S_w(f) \int_0^H C_p^2(z)\Phi_j^2(z)V_0^2(z)\,dz \tag{76}$$

We will also assume that $C_p(z)$ can be taken out of the integral by using an averaged pressure coefficient, C_D, calculated as

$$C_D = \frac{1}{BH}\int_0^H \int_0^B C_p(z)\,dx dz \tag{77}$$

We, therefore, can write for the PSDF of the j-th modal response at the top

$$S_{yj}(H,f) = \Phi_j^2(H)(\rho C_D B_j)^2 |H_j(f)|^2 S_w(f) \int_0^H \Phi_j^2(z)V_0^2(z)\,dz \tag{78}$$

Similarly, for the reference system

$$S_{rj}(H,f) = \Phi_r^2(H)(\rho C_D B_j)^2 |H_{rj}(f)|^2 S_w(f) \int_0^H \Phi_r^2(z) V_0^2(z)\, dz \tag{79}$$

For Case 1, from Eq.74 and also using Eq.73, the ratio of the top-story RMS responses $k_{1j}(H)$ becomes

$$k_{1j}(H) = \frac{\Phi_j(H)}{\Phi_r(H)} \cdot \frac{M_r^*}{M_j^*} \cdot \left[\frac{\int_0^H \Phi_j^2(z) V_0^2(z) dz}{\int_0^H \Phi_r^2(z) V_0^2(z) dz} \right]^{1/2} \tag{80}$$

6.2.2. Case 2: Pressures are fully correlated

If the pressures are fully correlated, the coherence function is unity, that is

$$Coh(x_1, z_1, x_2, z_2, f) = 1 \tag{81}$$

The PSDF of the generalized force (Eq.40) then becomes

$$S_{F_j^*}(f) = (\rho B_j)^2 S_w(f) \left[\int_0^H C_p(z) \Phi_j(z) V_0(z)\, dz \right]^2 \tag{82}$$

Using the same approximation as in Case 1 for $C_p(z)$, we can write for the PSDF of the j-th modal response at the top

$$S_{yj}(H,f) = \Phi_j^2(H)(\rho C_D B_j)^2 |H_j(f)|^2 S_w(f) \left[\int_0^H \Phi_j(z) V_0(z)\, dz \right]^2 \tag{83}$$

and similarly for the reference system

$$S_{rj}(H,f) = \Phi_r^2(H)(\rho C_D B_j)^2 |H_{rj}(f)|^2 S_w(f) \left[\int_0^H \Phi_r(z) V_0(z)\, dz \right]^2 \tag{84}$$

The ratio of the RMS responses, k_{2j}, becomes

$$k_{2j}(H) = \frac{\Phi_j(H)}{\Phi_r(H)} \cdot \frac{M_r^*}{M_j^*} \cdot \frac{\int_0^H \Phi_j(z) V_0(z) dz}{\int_0^H \Phi_r(z) V_0(z) dz} \tag{85}$$

As stated earlier, since the peak factors for the modal response and the corresponding reference system response are equal, these ratios are also valid for the peak responses. Therefore, the peak value of the j-th modal response at the top, $\max_t y_j(H,t)$, can be calculated in terms of the response ratio and the peak response of the reference system as

$$\max_t y_j(H,t) = k_j(H) \max_t y_r(H,t) \tag{86}$$

Since we defined $\max_t y_r(H,t)$ as the spectral response (Eq. 68), we can calculate the peak modal response as

$$\max_t y_j(H,t) = k_j(H) D(f_{0j}) \tag{87}$$

The total peak response can be approximated by combining peak modal responses. If SRSS (square-root-of-sum-of-squares) method is used for the combination, the total peak response becomes

$$\max_t y(H,t) = \left[\sum_{j=1}^{n} \left[\max_t y_j(H,t)\right]^2\right]^{1/2} = \left[\sum_{j=1}^{n} k_j^2(H) D^2(f_{0j})\right]^{1/2} \tag{88}$$

The equations for accelerations are similar. Since the relationship between accelerations and displacements is a function of frequency only (see Eq.47), the ratios k_{1j} and k_{2j} calculated for displacements are also valid for the accelerations. Therefore, we can calculate the peak top-story acceleration for the j-th mode, $\max_t a_j(H,t)$ in terms of the spectral acceleration of the reference system as

$$\max_t a_j(H,t) = k_j(H) A(f_{0j}) \tag{89}$$

The total peak acceleration is obtained by combining the peak modal accelerations as in Eq.88.

For a given building, the value of $k_j(z)$ is somewhere between $k_{1j}(z)$ and $k_{2j}(z)$. We have no way of knowing the exact values without explicitly incorporating the correlation structure of the wind. Therefore, an approximation needs to be made regarding which value to use for $k_j(z)$. For the first mode, the two values would be very close since the first mode shape in most buildings is almost a straight line, the same as that of the reference building. For higher modes, the ratio $k_{1j}(z)$ would always be larger than the ratio $k_{2j}(z)$, because the value of the integral $\int \Phi_j^2(z) V_0^2(z) dz$ is always larger than that of $\int \Phi_j(z) V_0(z) dz$ (the negative portions of mode shapes become positive in the first integral due to the square), whereas the values for the integrals $\int \Phi_r^2(z) V_0^2(z) dz$ and $\int \Phi_r(z) V_0(z) dz$ are always close.

Therefore, for higher modes $k_{1j}(z)$ can be considered as the upper bound, while $k_{2j}(z)$ is the lower bound. We suggest that an average value calculated as

$$k_j = \frac{k_{1j} + k_{2j}}{2} \tag{90}$$

is an appropriate one.

7. MODIFICATION OF EXISTING COMPUTER PROGRAMS

There is a large number of commercially available computer programs that can perform free vibration analysis. These programs can easily be extended to perform dynamic wind analysis by using the spectral analysis method presented above. In order to do this, we first have to generate a set of response spectra that includes spectral curves for different meteorological (e.g., mean wind velocities, turbulence levels, etc.), and structural (e.g., damping, width, height) conditions, as will be shown in the next section.

To estimate the dynamic wind response of a given building, we determine the natural frequencies, mode shapes, and generalized masses of the building by performing free vibration analysis. We then add a subroutine to the program to compute the ratios $k_{1j}(z)$ and $k_{2j}(z)$ and the average ratio $k_j(z)$ from Eqs.80, 85, and 90 for the velocity model selected. Note that only the shape, not the exact amplitudes, of the velocity profile is required in the calculations. The mode shape and the generalized mass for the reference system are given by Eqs.60 and 62. For each modal frequency and damping we take the spectral amplitude from the corresponding response spectra, and multiply it by the modal participation factor to obtain peak modal responses. We then combine the peak modal responses according to Eq.88 to obtain the total peak response.

8. EXAMPLES FOR WIND RESPONSE SPECTRA

In this section we develop a set of displacement and acceleration response spectra for a location assumed to be the center of a city. We consider three wind velocities, three building heights, three height-to-width ratios, and two damping ratios, resulting in $3 \times 3 \times 3 \times 2 = 54$ spectral curves for the displacements and accelerations. The frequency range used in the spectra is 0.1 Hz to 2.0 Hz with 0.1 Hz increments (20 values).

For the wind velocity structure, we assume the velocity profile and the PSDF suggested by Simiu (1973, 1974). The three mean wind velocities considered, at the reference height $z_r = 10$ $m.$, are $V_0(10) = 50$, 80, and 100 km/h. The roughness length, z_0 (Eq.3) was chosen 0.5 $m.$, a value representative of a city center. The friction velocity u_* for each $V_0(10)$ was calculated from Eq.6. The velocity spectrum used corresponds to a turbulence level, such that $\sigma_w^2 = 6\,u_*^2$. The pressure coefficient taken as $C_p(z) = 1.3$, which is assumed

to be the sum of the pressure coefficient on the front face (taken as 0.8), and the suction coefficient on the back face (taken as 0.5). It is assumed that this value represents the averaged value over the building (i.e., $C_D = C_p(z) = 1.3$ in Eq.77). The exponential decay coefficients of the coherence function (Eq.42) were chosen as $C_x = 16$ and $C_z = 10$. The mass density of the air is $\rho = 1.25\ kg/m^3$.

As for the structural parameters, we consider three heights, $H = 100, 200, 300\ m.$, and for each height, three height-to-width ratios, $H/B = 2, 4, 6$. The damping ratios used are 0.02 and 0.05. We also assumed unit mass per unit height. Since only alongwind direction forces and displacement are considered, the third dimension of the building (i.e., the depth) is not needed in the calculations.

For every combination of wind and structural parameters given above, the peak displacement and acceleration at the top of the building were calculated for frequencies from 0.1 to 2.0 Hz with 0.1 Hz intervals. The resulting spectral curves are plotted in Figs. 4 through 7. Figs. 4.a-c show the displacement spectra for 2-percent damping for for $V_0(10) = 50, 80$, and $100\ km/h$, respectively, whereas Figs. 5.a-c show the same for 5-percent damping. Corresponding curves for the acceleration spectra are given in Figs. 6.a-c and Figs. 7.a-c for 2-percent and 5-percent damping ratios. The spectra are plotted on a log-log scale to be consistent with the convention used for earthquake excitations. As the figures show, the displacement spectra are all straight lines. Recall that these spectra are for the displacement due to dynamic wind forces only. The acceleration spectra differ slightly from a straight line.

9. USE OF WIND TUNNELS FOR WIND RESPONSE SPECTRA

The wind response spectra in the previous section were developed by using an analytical approach. A more accurate spectra can be developed in wind tunnels. The procedure suggested here to develop spectra is based on a reference building, which is a rigid block with rotational base spring and damper. This building can easily be modeled in a wind tunnel by using a flexible base plate. By changing the flexibility of the base plate, the response spectra can be obtained for a given location and a building with specified dimensions. By testing various buildings with different outside dimensions and damping ratios, and also considering different wind conditions, a data base for wind response spectra can be generated in the laboratory. It may be argued that modeling the roughness around the building is an important and critical part of the wind tunnel tests, and it is unique for each building. However, a generic roughness model for a given location can be approximated, since wind spectra will be used for preliminary design purposes, rather than exact response estimations.

10. COMFORT SPECTRA

Occupant discomfort due to wind-induced motions has long been recognized as one of the major problems in high-rise buildings (Hansen, et. al., 1973). The discomfort is mainly due to excessive low-frequency accelerations in the upper stories of buildings. The critical values of maximum acceleration for human comfort are available from experimental studies (NBCC, 1985). For a given building height and width, and wind structure, we can plot the acceleration response spectra. The intersection of the spectra with the straight line representing the critical acceleration gives the critical frequency of the building. This is schematically shown in Fig. 8. In order not to have human discomfort, the building should be designed to have a frequency higher than the critical frequency. If we determine critical frequency by using this approach for a range of building heights, we can then construct an interaction curve showing the building height versus critical frequency for a specifed location. We will call this interaction curve the *comfort spectrum.* The left side of this curve (i.e., the lower frequency side) represents the uncomfortable side. We should select building height and frequency to stay on the right side of the curve.

To give an example, a set of comfort spectra for the reference building was developed by considering the same set of values used for the development of response spectra in section 8. To make the values realistic, we used $m = 150. \times B^2\ kg/m$ for the mass per unit length instead of unit mass. The critical acceleration for human discomfort was taken as $0.005\mathbf{g}$, where $\mathbf{g}$ is the gravitational acceleration. The comfort spectra are plotted in Fig. 9 for 2-percent damping, and in Fig. 10 for 5-percent damping. Each spectra is composed of three points (corresponding to H =100, 200, and 300 m.), connected by straight lines.

11. JOINT DESIGN SPECTRA FOR WIND AND EARTHQUAKES

It is likely that for most buildings, either wind or earthquake will determine the design criteria for lateral loads. Since we now can draw the wind response spectra in the same way as the earthquake response spectra, we can easily plot them together superimposed on the same axes, and see which one dominates at each frequency. This allows the designer to determine which load is more critical for his building without doing any analysis.

An important drawback in this approach is that in any given location the probability of occurence of a large storm is not equal to the probability of occurence of a large earthquake. Therefore, a straightforward comparison of the two spectra is not appropriate. We can incorporate the probabilities of occurences in the spectra by using appropriate weighting factors for each spectra, or we can scale each spectra in a probabilistic manner and compare them for a specified exceedance (e.g., 90-percent) level.

We will investigate this topic in detail after we complete the second phase of the

study on wind spectra, where we will develop wind response spectra for across-wind vibrations. The reason for this is that for some buildings across-wind vibrations may dominate the along-wind vibrations. In such cases we need to compare across-wind spectra with earthquake spectra.

12. SUMMARY AND CONCLUSIONS

We have presented a response spectrum technique to estimate wind-induced dynamic response (displacements and accelerations) of high-rise buildings. The method presented is parallel to that used for earthquake excitations. At this phase of the research, we consider only along-wind direction forces and vibrations. We will consider across-wind direction response in the second phase of the research.

We develop wind response spectra for a reference building, defined as a single-degree-of-freedom rectangular rigid block, with a rotational base spring and a damper. The wind response spectrum is obtained as the peak response of the reference building for a range of frequencies. We present 54 response spectra considering different combinations of wind and structural configurations. We show that, for any given building, we can calculate peak modal responses in terms of those of the reference building. We obtain the total peak response of the building by combining peak modal responses.

We have also introduced the concept of comfort spectra. For a given building height, we plot the acceleration response spectrum, and observe the building frequency corresponding to the critical acceleration for human discomfort. By doing this for a range of building heights, we can construct an interaction curve showing the building height versus critical frequency. We call this interaction curve the comfort spectrum. We present a set of examples for comfort spectra.

We conclude by discussing the development of a joint design spectrum for wind and earthquakes loads. We will do a more detailed study on this topic after we complete the second phase of the reserach, where we will develop response spectra for across-wind vibrations.

REFERENCES

ANSI (1982). American National Standard, Minimum design loads for buildings and other structures, *American National Standards Institute, Inc.* , New York, NY, ANSI A58.1-1982.

Cevallos-Candau, P.J. (1980). The commonality of earthquake and wind analysis, *Ph.D. Thesis*, Department of Civil Engineering, University of Illinois, Urbana, Illinois.

Davenport, A. G.(1961). The application of statistical concepts to the wind loading of structures, *Proc., Inst. of Civil Eng.*, London, Vol. 19, pp. 449–472, 1961.

Davenport, A. G. (1964). The distribution of largest value of a random function with application to gust loading, *Proc., Inst. of Civil Eng.*, London, Vol. 28, pp. 187–196, 1964.

Hansen, R.L., J.W. Reed, and E.H. Vanmarcke (1973). Human response to wind induced motion of buildings, *Engineering Journal*, American Institute of Steel Construction, July 1973.

Hurty, W.C. and M.F. Rubinstein (1964). *Dynamics of Structures*, Prentice-Hall, Inc., Englewood Cliffs, NJ.

Lin, Y. K. (1976). Probabilistic Theory of Structural Dynamics, *Robert E. Krieger Publishing Company*, Huntington, New York, 1976.

NBCC (1985). National Building Code of Canada, *National Research Council of Canada*, Ottawa, Canada.

Newmark, N.M. (1966). Relation between wind and earthquake response of tall buildings, *proceedings*, 1966 Illinois Structural Engineering Conference, University of Illinois, Urbana, Ill.

Safak, E. and D.A. Foutch (1980). Vibration of buildings under random wind loads, *Department of Civil Engineering*, University of Illinois, SRS No. 480, Urbana, Illinois, May 1980.

Şafak, E. and D.A. Foutch (1987). Coupled vibrations of rectangular buildings subjected to normally-incident random wind loads, *Journal of Wind Engineering and Industrial Aerodynamics*, 26, pp.129-148.

Simiu, E. (1973). Logarithmic profiles and design wind speeds, *Jour. of Eng. Mech. Div., ASCE*, v.99, EM5, October 1973, pp.1073-1083.

Simiu, E. (1974). Wind spectra and dynamic alongwind response, *Jour. of Struc. Div., ASCE*, v.100, ST9, Sept. 1974, pp. 1877–1910.

Simiu, E. and R.H. Scanlan (1978). Wind Effects on Structures, an Introduction to Wind Engineering, *John Wiley and Sons*, New York, 1978.

Vickery, B. J. (1971). On the reliability of gust loading factors, *Civil Engineering Transactions*, pp. 1–9, April 1971.

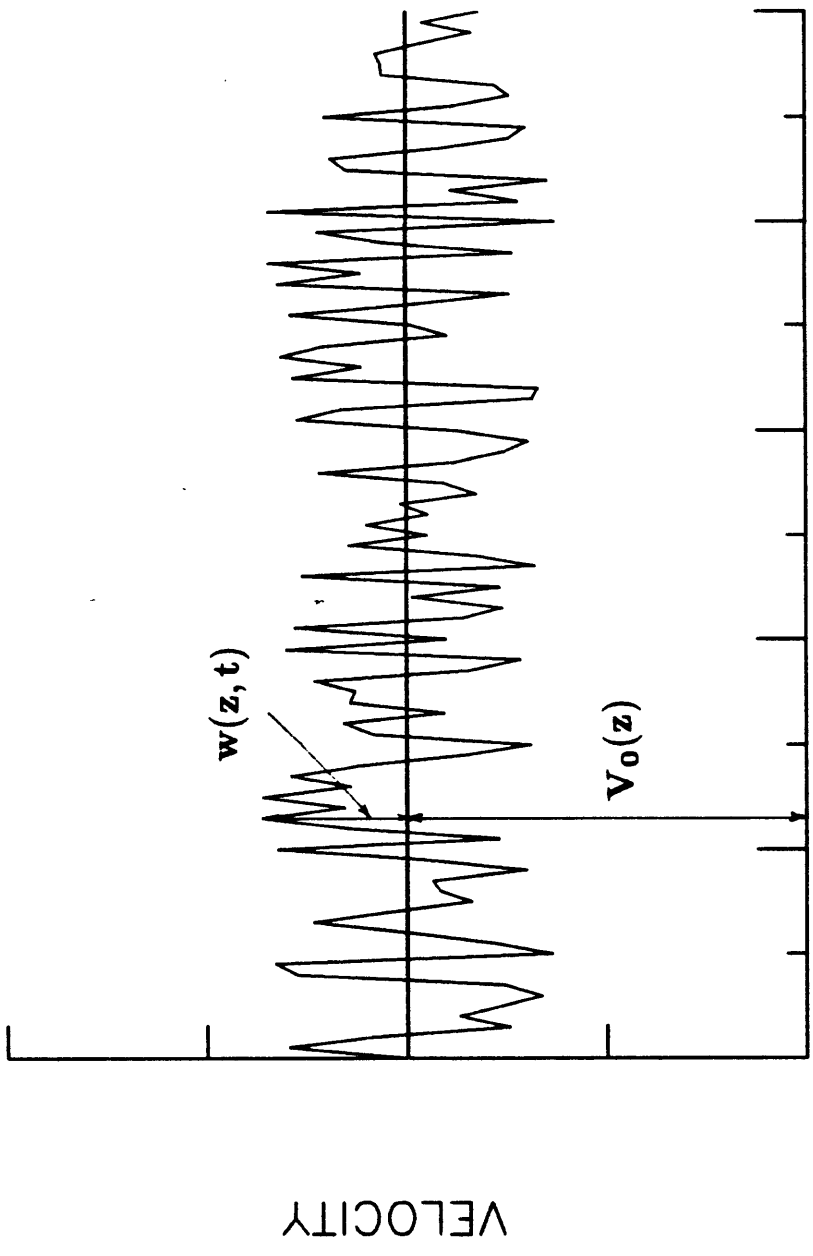

FIG. 1. Mean and fluctuating components of wind velocity.

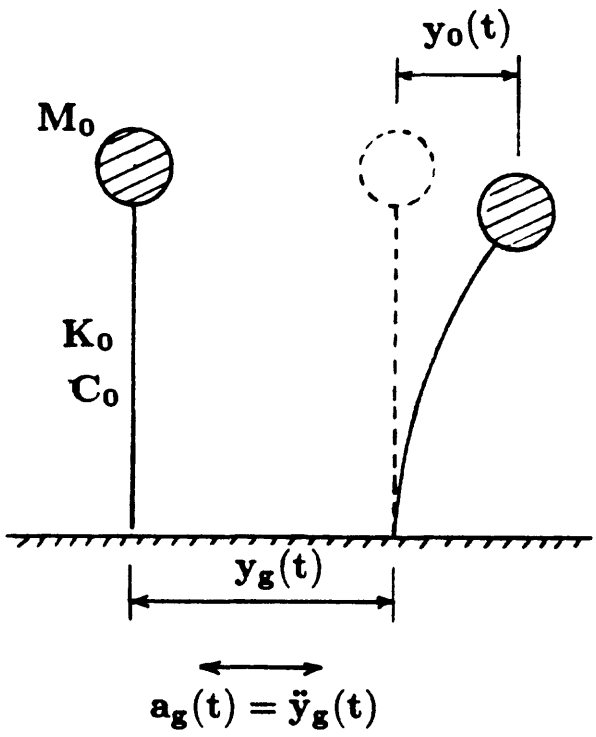

FIG. 2. Single-degree-of-freedom damped oscillator subjected to base acceleration.

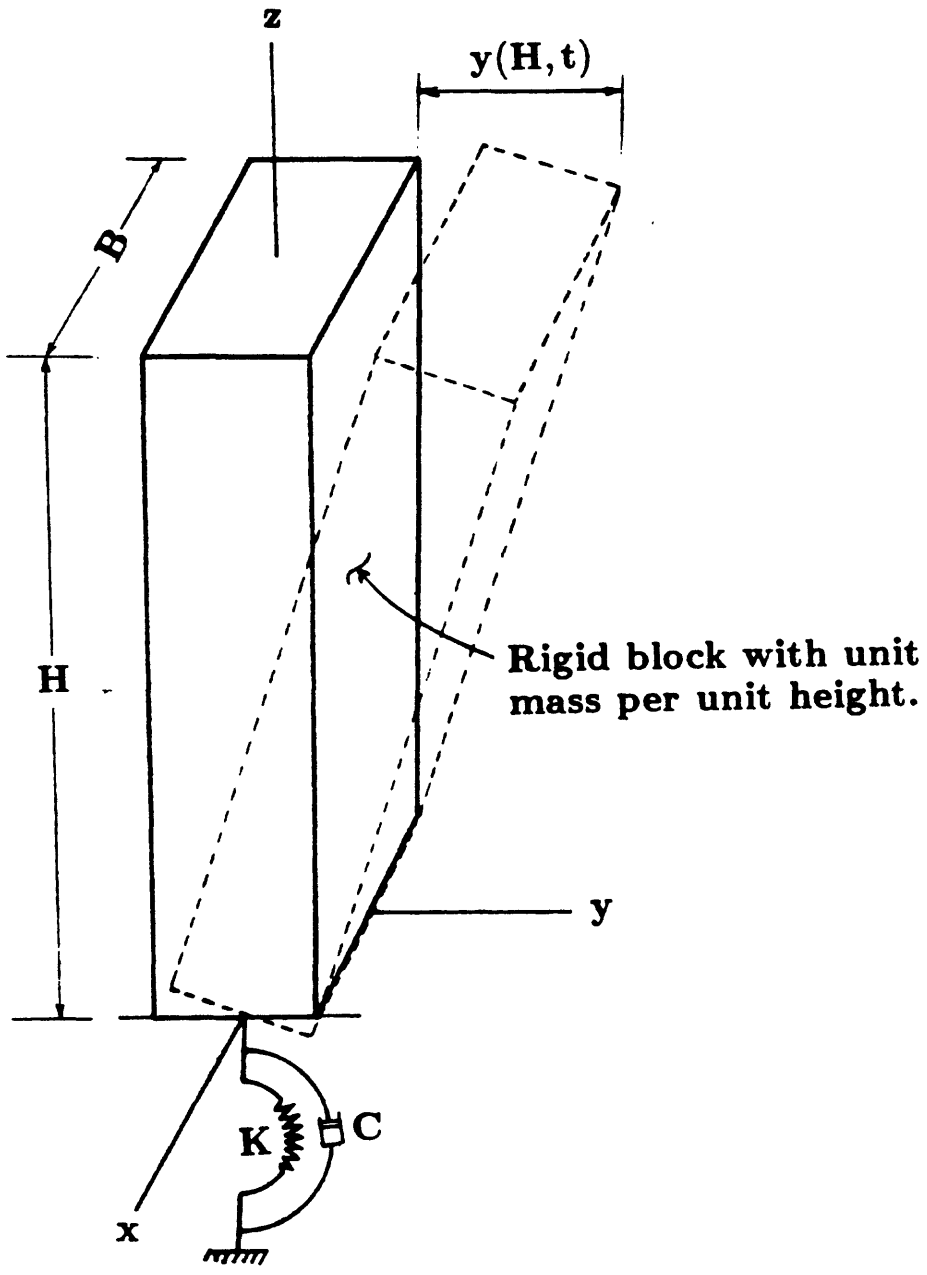

FIG. 3. Schematic view of the single-degree-of-freedom reference building used to generate response spectra.

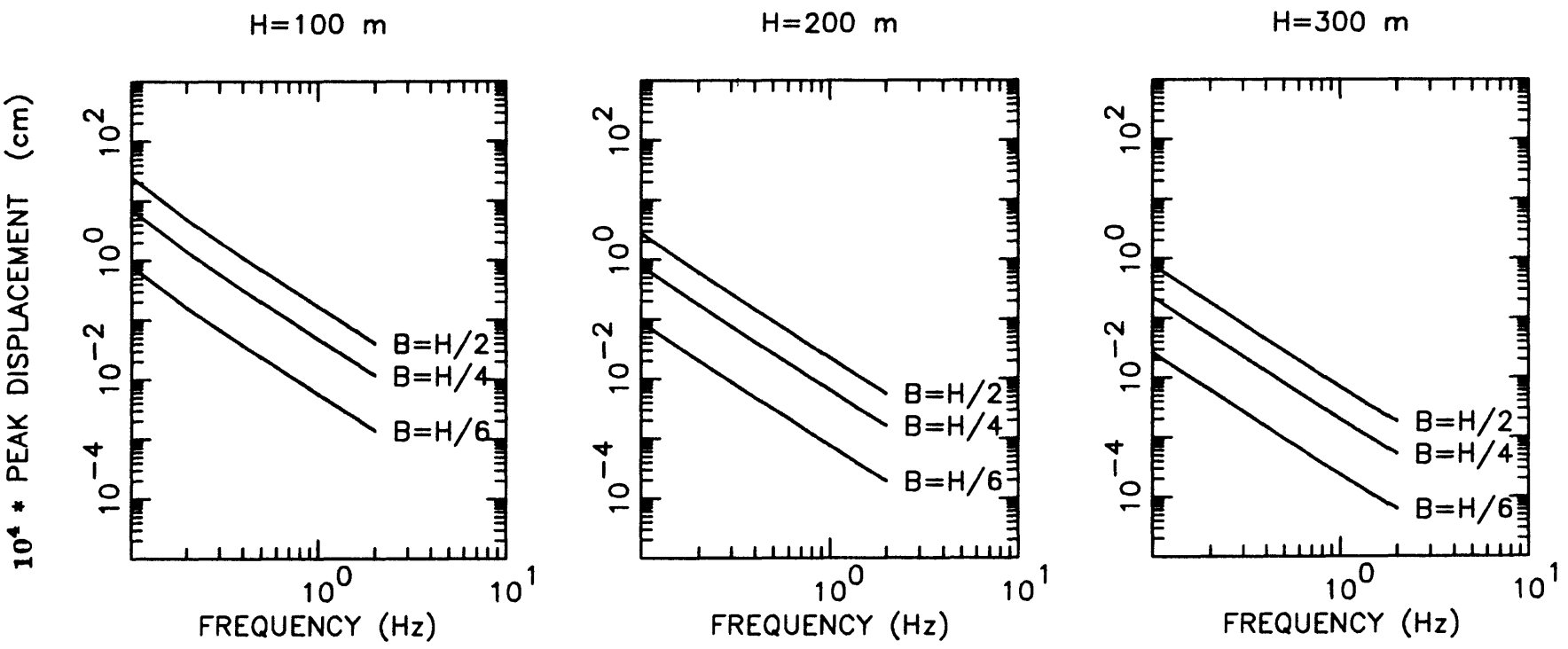

FIG. 4.a. Displacement response spectra for the reference building for H = 100, 200, and 300 m.: Unit mass per unit length; 2-percent damping; center of a city with $V_0(10) = 50\ km/h$.

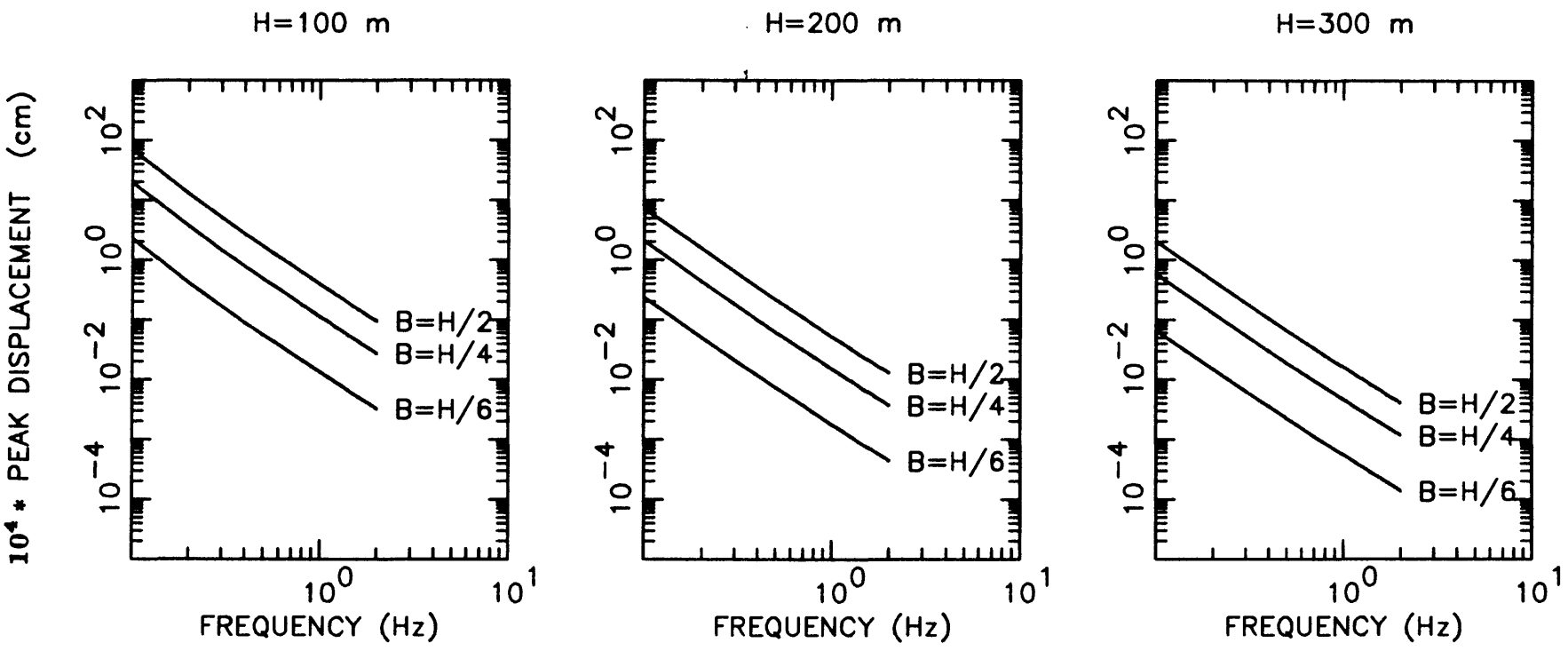

FIG. 4.b. Displacement response spectra for the reference building for H = 100, 200, and 300 m.: Unit mass per unit length; 2-percent damping; center of a city with $V_0(10) = 80$ km/h.

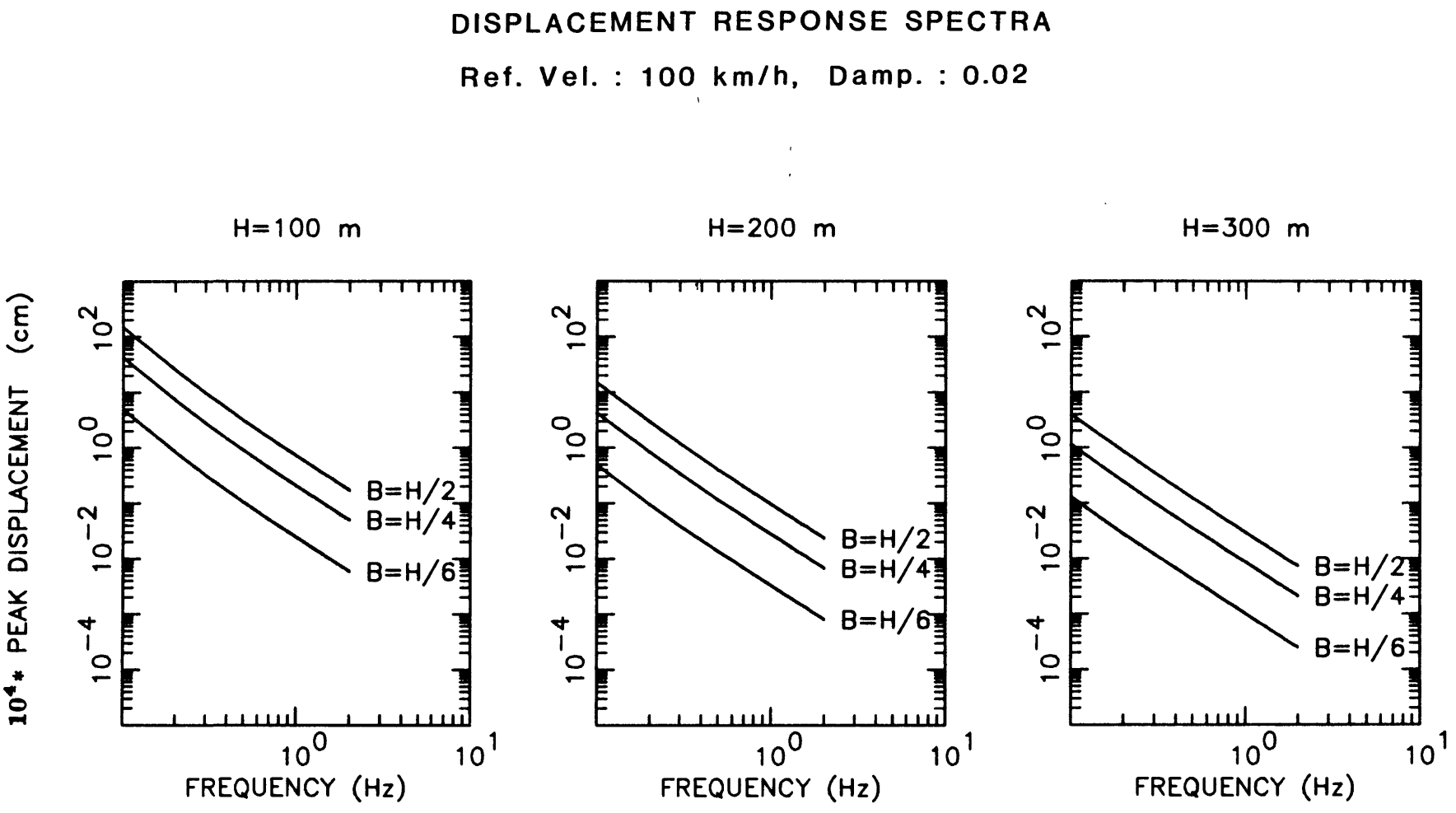

FIG. 4.c. Displacement response spectra for the reference building for H = 100, 200, and 300 m.: Unit mass per unit length; 2-percent damping; center of a city with $V_0(10) = 100\ km/h$.

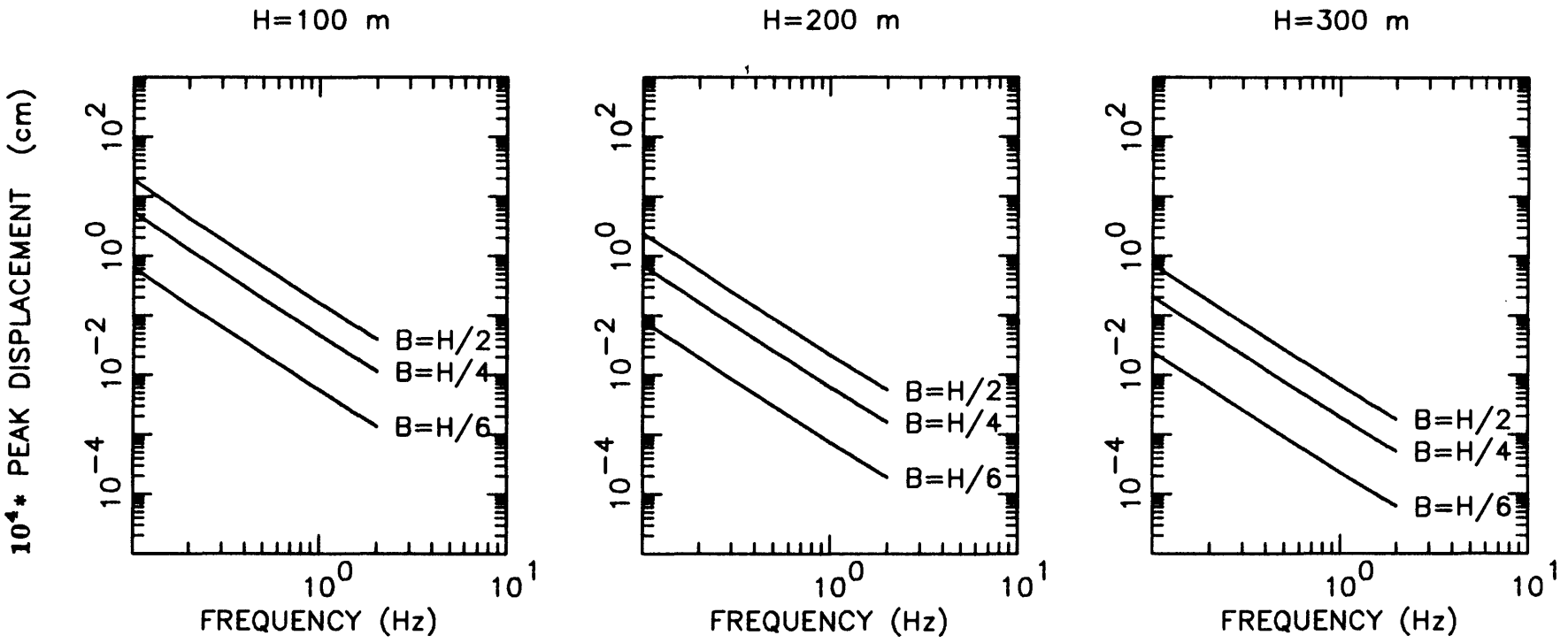

FIG. 5.a. Displacement response spectra for the reference building for H = 100, 200, and 300 m.: Unit mass per unit length; 5-percent damping; center of a city with $V_0(10) = 50$ km/h.

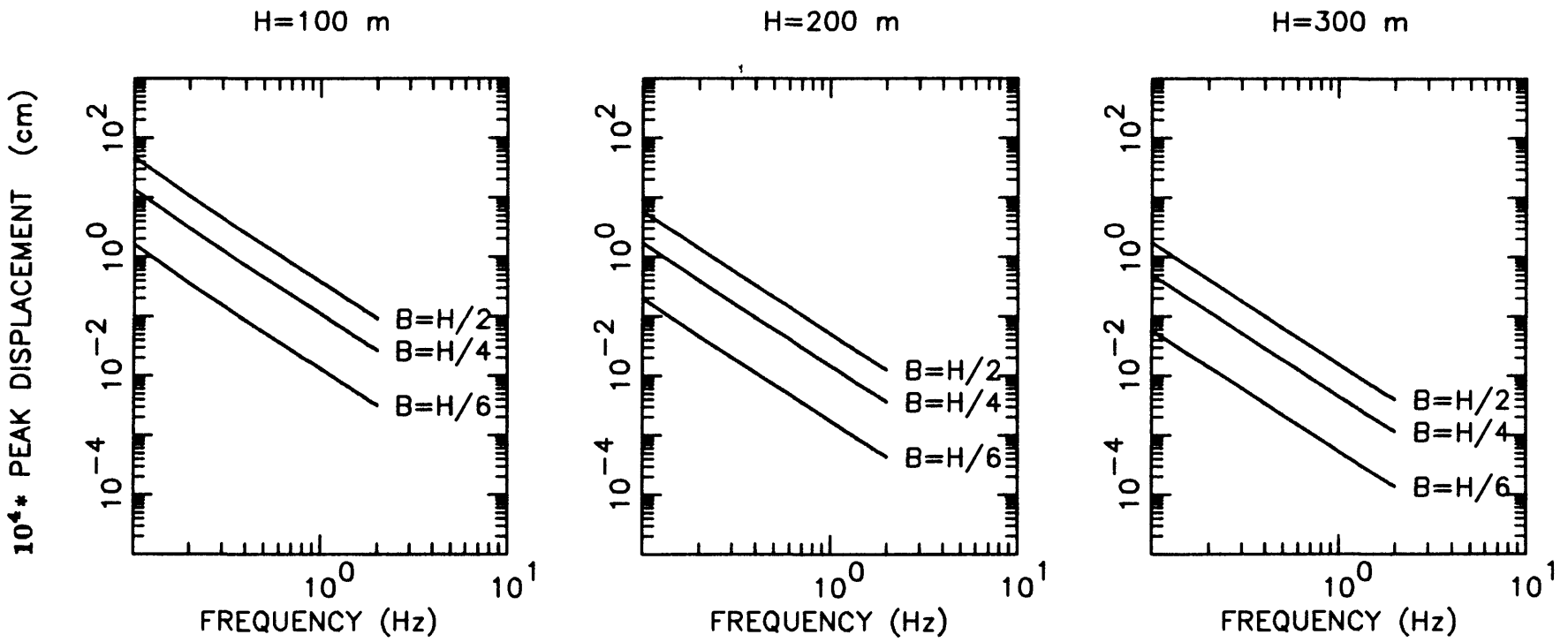

FIG. 5.b. Displacement response spectra for the reference building for H = 100, 200, and 300 m.: Unit mass per unit length; 5-percent damping; center of a city with $V_0(10) = 80\ km/h$.

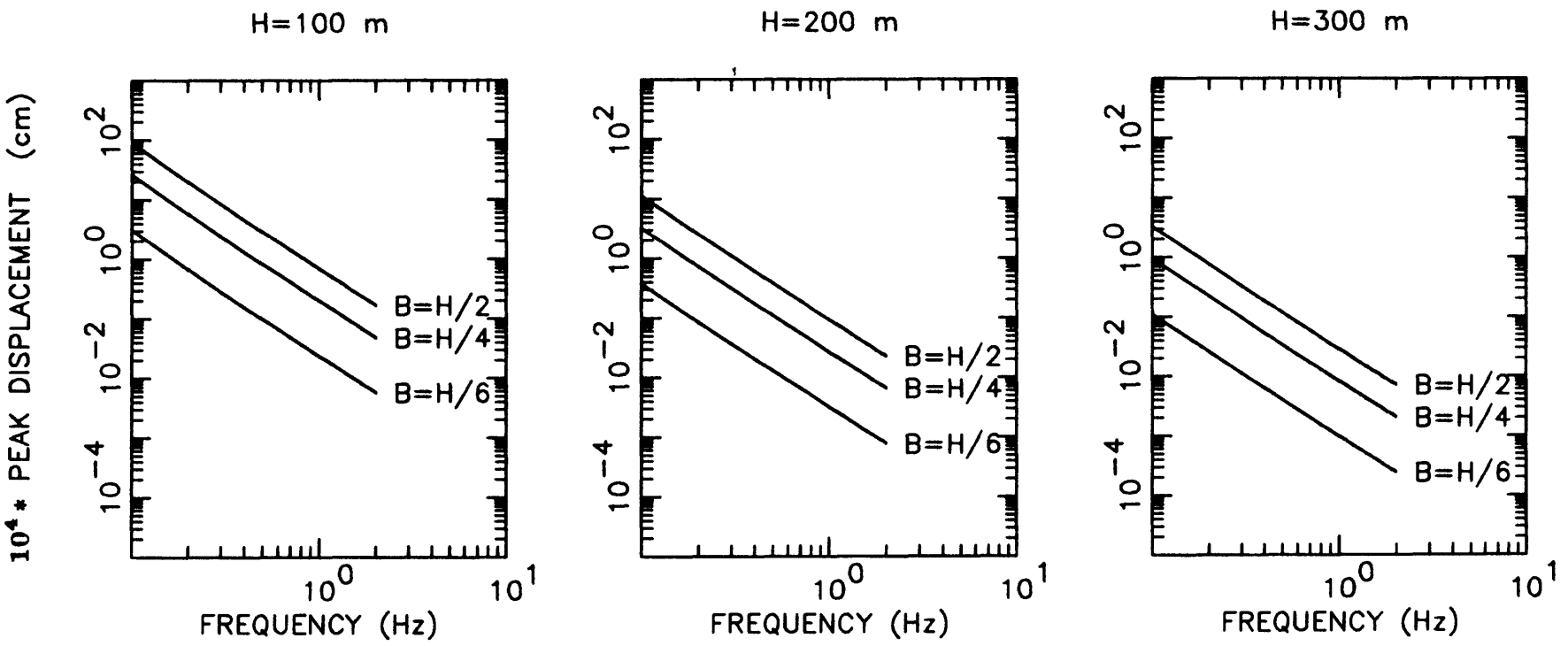

FIG. 5.c. Displacement response spectra for the reference building for H = 100, 200, and 300 m.: Unit mass per unit length; 5-percent damping; center of a city with $V_0(10) = 100\ km/h$.

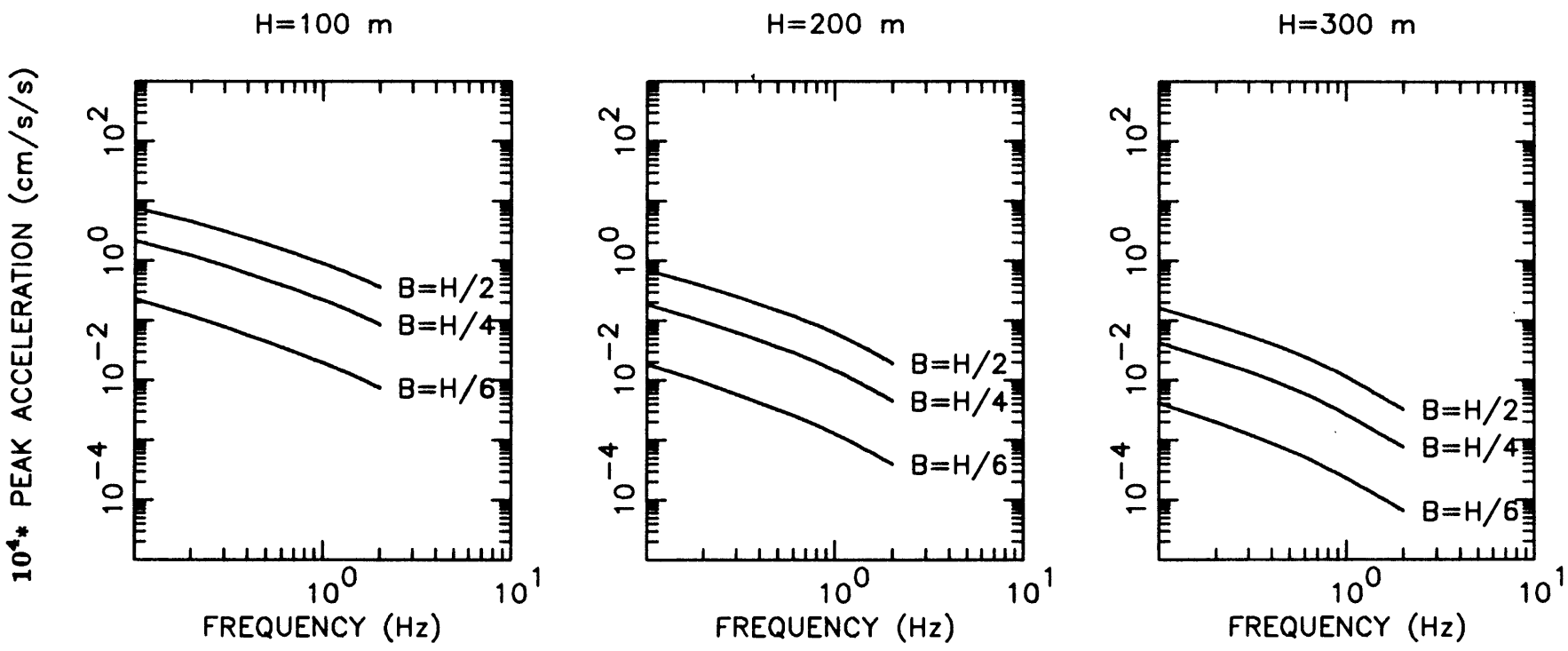

FIG. 6.a. Acceleration response spectra for the reference building for H = 100, 200, and 300 m.: Unit mass per unit length; 2-percent damping; center of a city with $V_0(10) = 50\ km/h$.

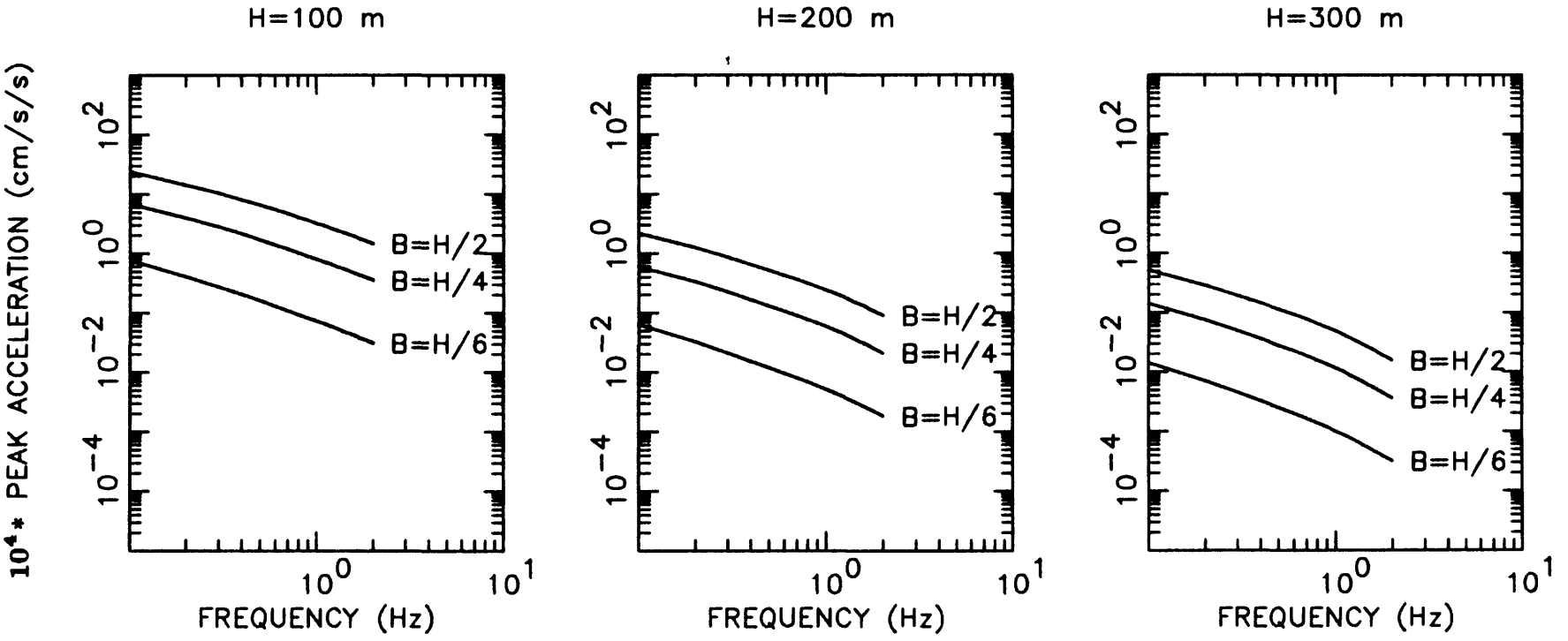

FIG. 6.b. Acceleration response spectra for the reference building for H = 100, 200, and 300 m.: Unit mass per unit length; 2-percent damping; center of a city with $V_0(10) = 80\ km/h$.

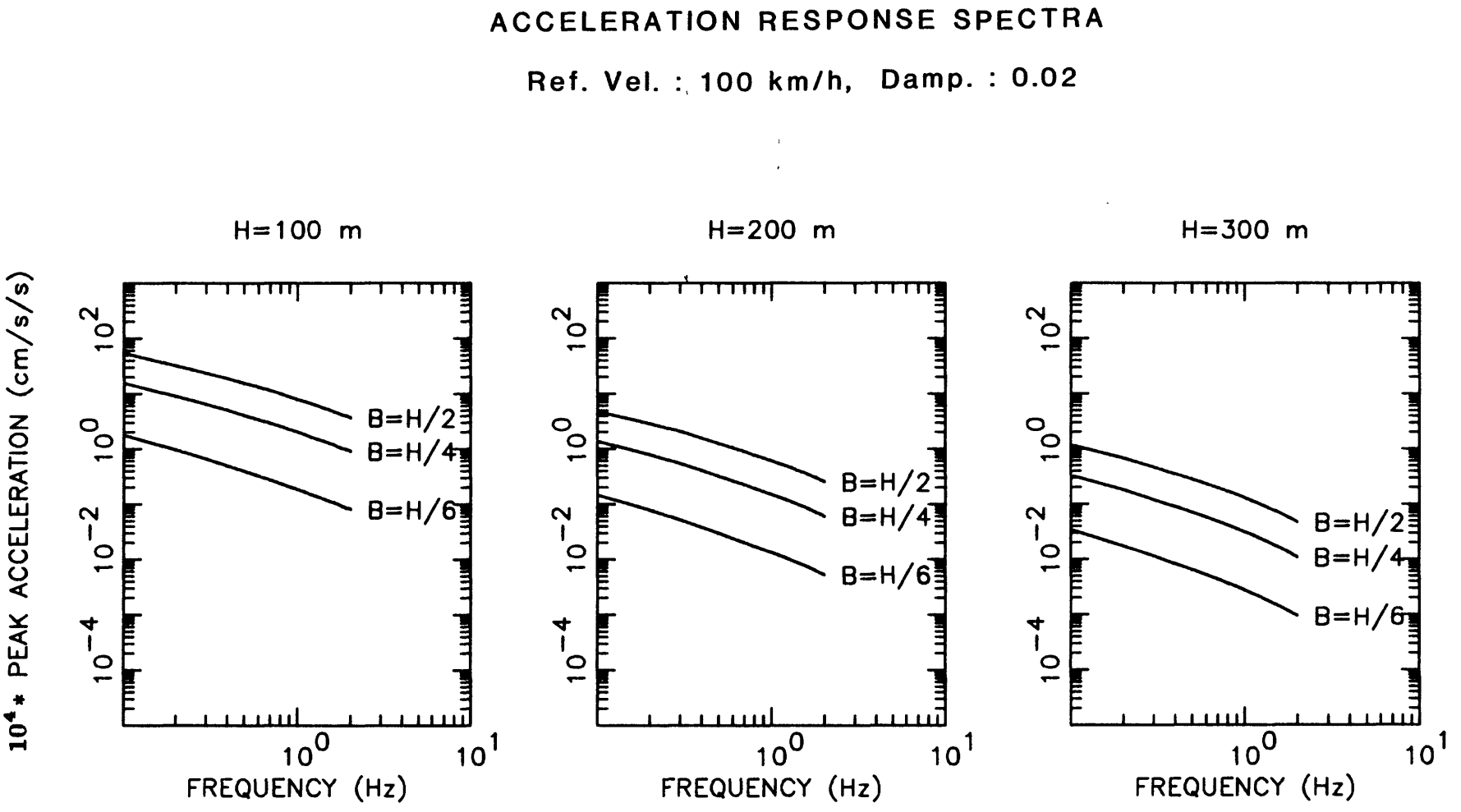

FIG. 6.c. Acceleration response spectra for the reference building for H = 100, 200, and 300 m.: Unit mass per unit length; 2-percent damping; center of a city with $V_0(10) = 100\ km/h$.

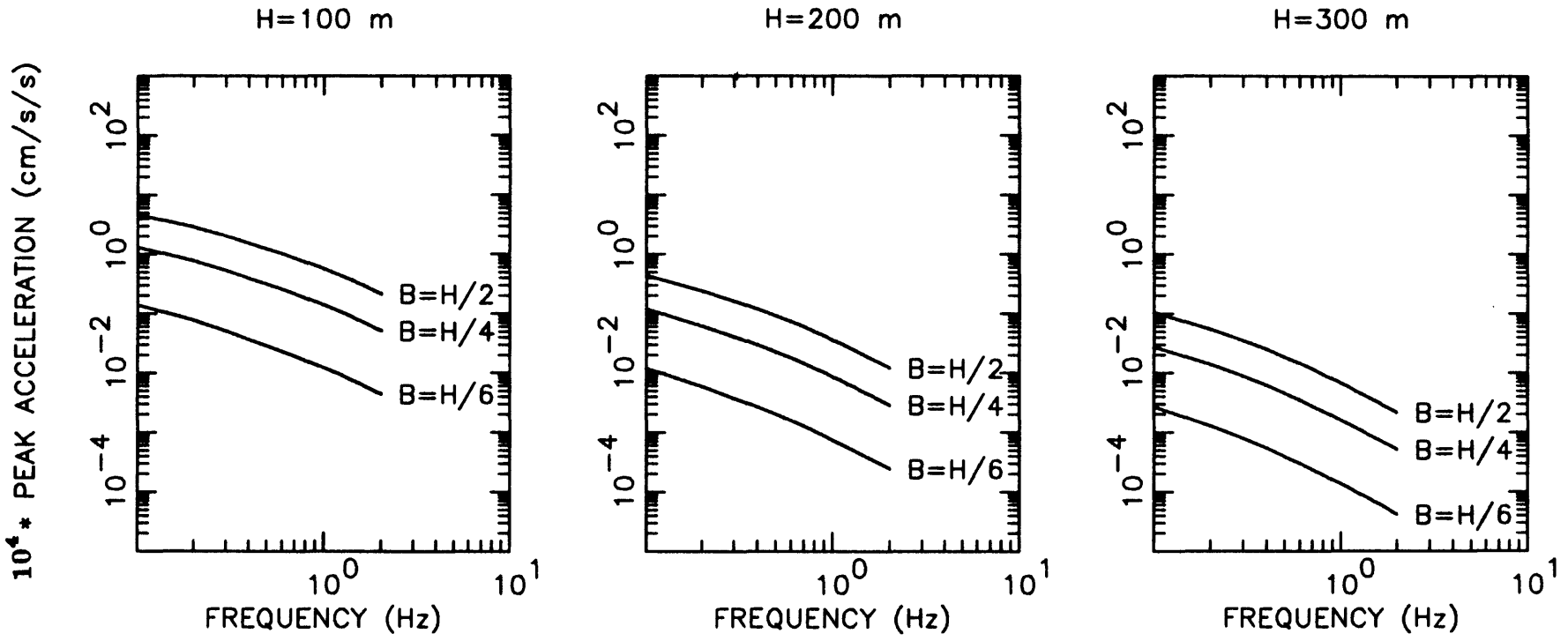

FIG. 7.a. Acceleration response spectra for the reference building for H = 100, 200, and 300 m.: Unit mass per unit length; 5-percent damping; center of a city with $V_0(10) = 50\ km/h$.

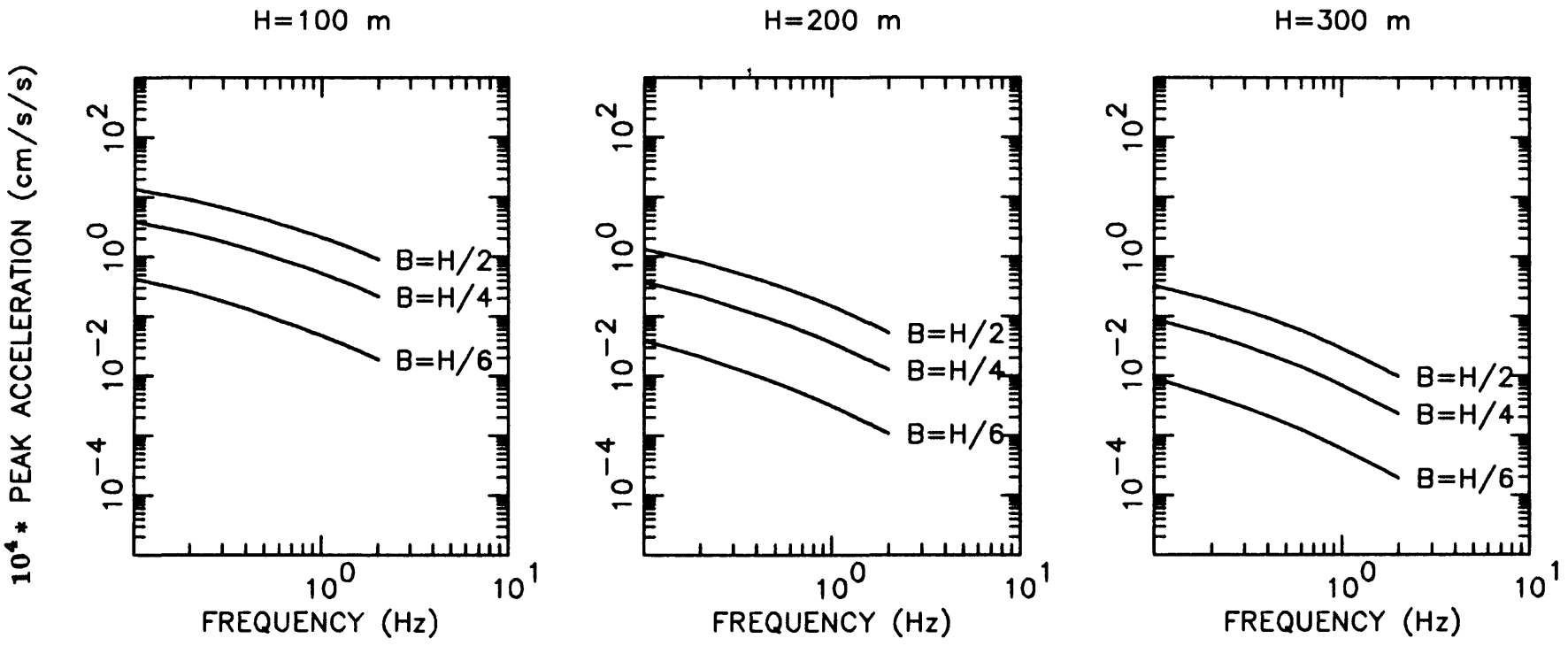

FIG. 7.b. Acceleration response spectra for the reference building for H = 100, 200, and 300 m.: Unit mass per unit length; 5-percent damping; center of a city with $V_0(10) = 80$ km/h.

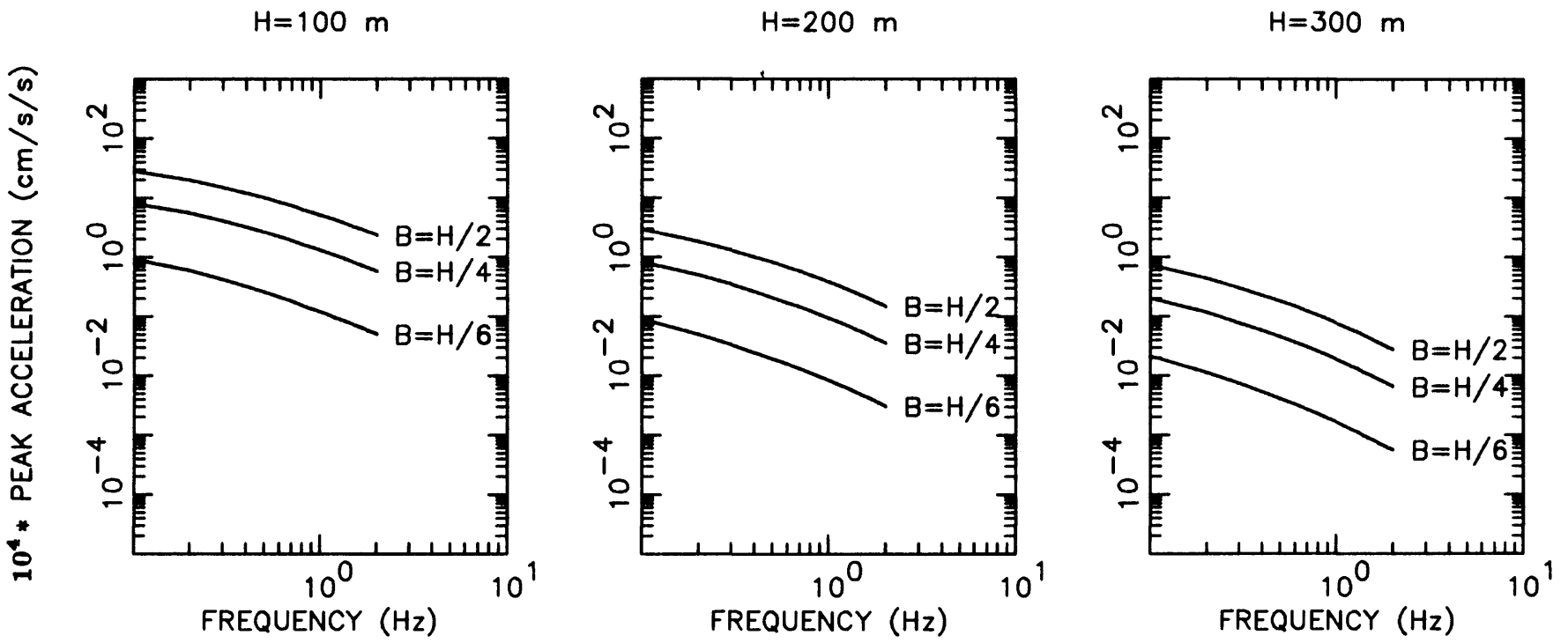

FIG. 7.c. Acceleration response spectra for the reference building for H = 100, 200, and 300 m.: Unit mass per unit length; 5-percent damping; center of a city with $V_0(10) = 100\ km/h$.

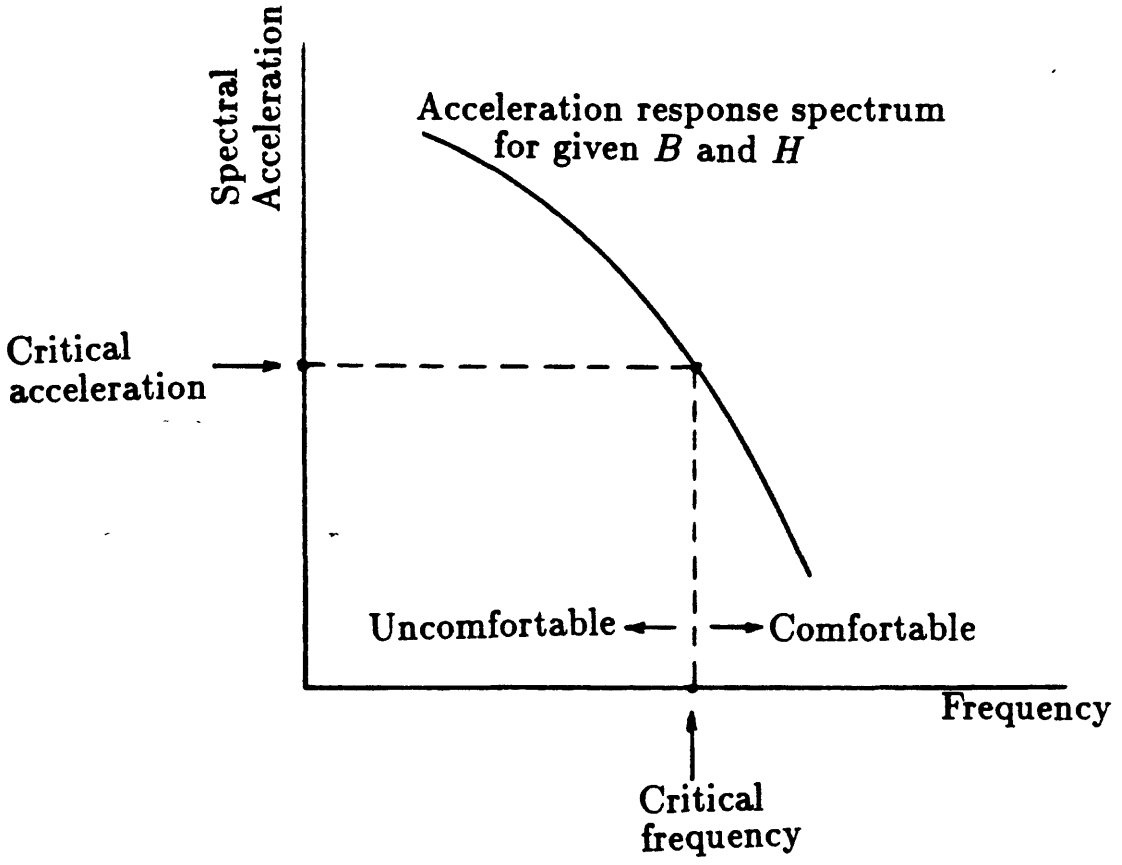

FIG. 8. Development of comfort spectrum.

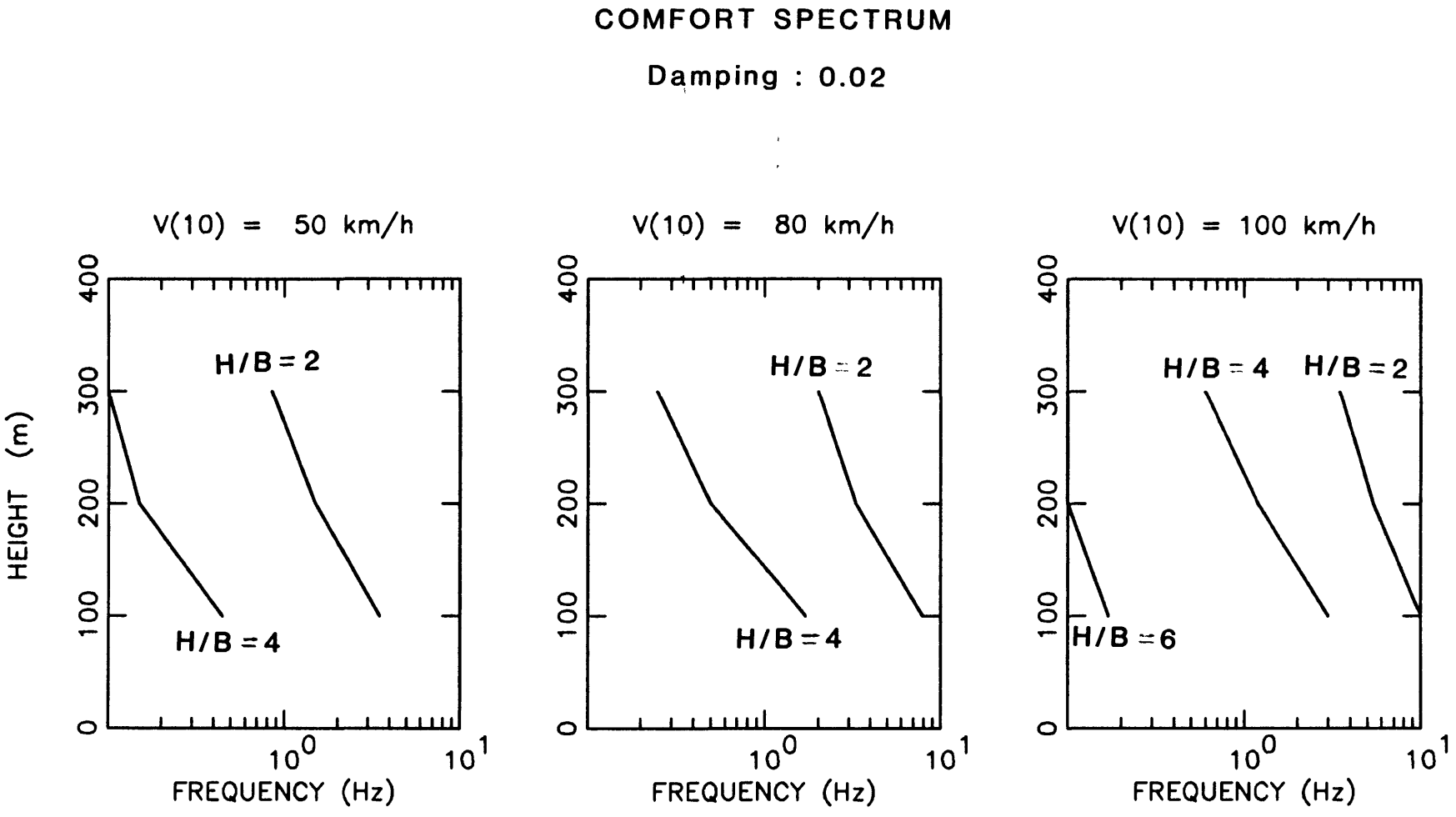

FIG. 9. Comfort spectrum for 2-percent damping (mass per unit length= $150 \times B^2\, kg/m$**; center of a city).**

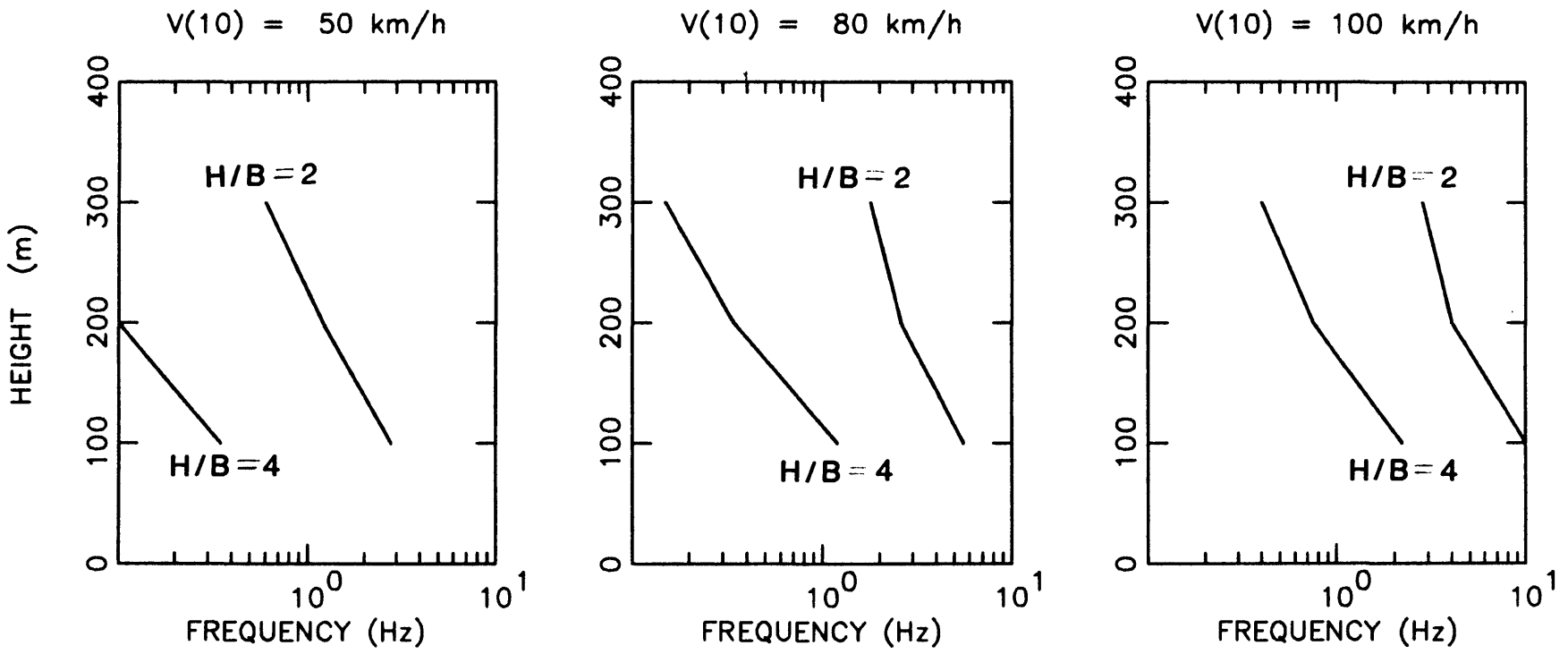

FIG. 10. Comfort spectrum for 5-percent damping (mass per unit length= $150 \times B^2\, kg/m$**; center of a city).**